Synthesis and Characterization of Humic Acid Coated Magnetite Nanoparticles for the Removal of methylene blue from Aqueous Solutions

By: Gietu Yirga Abate

A Thesis Submitted to the Department of Applied Chemistry

In Partial Fulfillment of the Requirements for the Degree of Master of Science in Applied Chemistry (Industrial Chemistry)

School of Applied Natural Science

Office of Postgraduate

Adama Science and Technology University

August, 2018

Adama, Ethiopia

Synthesis and Characterization of Humic Acid Coated Magnetite Nanoparticles for the Removal of Methylene blue from Aqueous Solutions

By: Gietu Yirga Abate

Advisor: Eshetu Bekele (PhD)

Co-advisor: Tajudin Alansi (PhD)

A Thesis Submitted to the Department of Applied Chemistry

In Partial Fulfillment of the Requirements for the Degree of Master of Science in Applied Chemistry (Industrial Chemistry)

School of Applied Natural Science

Office of Postgraduate

Adama Science and Technology University

September, 2018

Adama, Ethiopia

Approval Sheet

BY

Name of student	Signature	Date

As thesis advisor, we hereby certify that we have read and evaluated this thesis paper under our guidance, by Gietu Yirga Abate entitled: **"Synthesis and characterization of Humic Acid Coated Magnetite Nanoparticles for the Removal of Methylene Blue from Aqueous Solutions** "and submitted in fulfillment of the requirement for Master of Science in Chemistry (Industrial Chemistry) complies with the regulation of the university and meets the accepted standards with respect to originality and quality of the desired work.

Major advisor	Signature	Date
Co-advisor	Signature	Date

As members of the board of examiners for the M.Sc. thesis open defense examination, we certify that we have read and evaluated the thesis paper prepared by Gietu Yirga Abate and examined the candidate. We recommended the thesis paper to be accepted as fulfillment for the requirements of the thesis guideline of Adama Science and Technology University.

Chair man	Signature	Date
Internal Examiner	Signature	Date
External Examiner	Signature	Date
Department Head	Signature	Date
School Dean	Signature	Date

DECLARATION

I hereby declare that the thesis entitled **synthesis and characterization of humic acid coated magnetite nanoparticles for the removal of methylene blue from aqueous solution** has been carried out by me under the supervision of Dr. Eshetu Bekele and Dr. Tajudin Alansi, during the year 2017/2018 as part of Master of Science Program in Industrial Chemistry. I further declare that this work has not been submitted to any other Universities or institutions for the award of any degree. All quotations and their sources are specifically acknowledged by means of references.

Name : Gietu Yirga Abate

Signature _____

This M.Sc. thesis has been submitted for examination with our approval as thesis advisors.

Advisor Name: Eshetu Bekele (PhD)

Signature _____

Co-advisor Name: Tajudin Alansi (PhD)

Signature _____

Date of Submission _____

DEDICATIONS

This thesis is dedicated to my beloved parents Yirga Abate and Weyzero Yemata Adugna and my beloved brothers Amare Yirga and Awoke Worku for nursing me with affection, unreserved assistance and for their dedicated encouragement in my academic carrier. I pray to God to rest their soul in peace.

Table of contents

Contents Page

Acknowledgements

First of all I would like to thank the Almighty God and his beloved mother Saint Virgin Mary for the unreserved and unconditional love, kindness and for keeping me in health, strength and courage in the entire period of this work.

Next, special thank and heartfelt appreciation goes to my best instructor and major advisor Dr. Eshetu Bekele for his unreserved support and guidance during thesis proposal writing, research work and thesis write up. His constructive criticism and comments from the initial conception to the end of this work is highly appreciated. I pay respect and express gratitude to him for his guidance, consistent supervision as well as suggestions in every phase of this research work.

I am deeply thankful to my co-advisor Dr. Tajudin Alensi and major advisor Dr. Eshetu Bekele, for their supply of the priceless and valuable chemicals (Humic acid) which made this research possible on time. I also acknowledge greatly Dr. Ananida Murssa for his help me for SEM-EDX characterization of my sample in Indian.

Also, I would like to acknowledge greatly Adama Science and Technology University for giving me M.Sc. free Sponsorship program. I would like to acknowledge the department of applied chemistry program in facilitating and encouraging all things to complete this program. I have also special thank to chemistry laboratory lab assistance Merriama Kufa For assisting me during UV visible spectroscopy analysis of laboratory work and all biology departments staff members for their support to use full laboratory area to conduct adsorption experiment.

Next I want to thank my family who were big sources of inspirations throughout my academic career with their valuable moral support and advice. I should not forget lovely my best sister Abebayehu Abebe Mamo and my best most relative brothers Enyew Tilahun, Getahun Abirham and Kebede Mamo for their supporting in different direction to me that brought me up to this success and for their encouragement and moral support during this study and finally I want to thanks all M.SC.students for their supports, comments and valuable information's to success this study.

Abstract

During the last few decades different methods were studied for the removal of dyes from industrial effluents as their disposal have toxic effects to humans, animals, plants and the aquatic organisms. Very recently magnetic nanoparticles (NPs) have been extensively used to remove this dye but to enhance its removal efficiency problem related to aggregation and oxidation of these nanoparticles in aqueous solution needs to be addressed .Therefore, the focus of this research was to address the problems by coating the NPs with polymeric materials like humic acid. Magnetite NPs were synthesized by co-precipitation method. Humic acid coated magnetite nanoparticles of labeled HAC-1(10:1ratio) and HAC-2 (20:1) were synthesized with the same method by varying the proportion of precursor magnetite and humic acid ratio (10:1 and 20:1).The chemical and physical characteristic of synthesized nanoparticles were characterized by Fourier transformed infrared spectroscopy (FTIR), X-ray diffraction spectroscopy, Scanning electron microscopy-energy dispersive x-ray spectroscopy (SEM-EDX) and UV-Vis DRS spectroscopy. The characterized nanoparticles were used for the removal of methylene blue from aqueous solution by adsorption mechanism. The effects of the contact time, dose of the adsorbent, pH, and initial dye concentration on the adsorption capacity were studied. The kinetics and adsorption isotherm were also studied. The crystal size of NPs calculated by Debye-Scherer equation were 9.17 nm, 12.65 nm and 11.5 nm for HAC-1, HAC-2and bare magnetite NPs, respectively. Both of the bare magnetite and the coated magnetite had cubic spinel structure and the spherical shaped morphology. The band gap energy of synthesize NPs were 3.24 eV, 3.2 eV and 3.18 Ev for Fe3O4 HAC-1 and HAC-2 respectivly.The results showed that the adsorption capacity for the dye increased by increasing the contact time, adsorbent dose and initial pH of the solution until reach to equilibrium but slightly decrease after equilibrium. However, it decreased with increasing the adsorbate (methylene blue) concentration. The adsorption kinetics was in good agreement with pseudo 2ndorder kinetic equation and the adsorption isotherm showed good fitting to Langmuir equation and the maximum adsorption capacity was 62 mg/g, 40 mg/g and 34.48mg/g for HAC-1 , HAC-2 and bare magnetite NPs respectively. The MB removal efficiency of HAC-1, HAC-2 and bare magnetite from aqueous solution were 99.5%, 97.6% and 95.8% respectively. The result clearly indicated the MB removal efficiency of magnetite nanoparticles from aqueous solution can be improved by coating with humic acid.

. Keyword: - Humic Acid, Methylene blue, Co-Precipitation, Magnetite Nanoparticles

List of Abbreviations and Acronyms

b	Langmuir Constant
c	Speed of Light
Ccp	Cubic Close Pack
C_e	Equilibrium Concentration
C_o	Initial Concentrations
SPIONPs	Supper magnetic iron oxide nanoparticles
C_t	Concentration at Any Time T
E_g	Band gap Energy
FTIR	Forier Transfer Infra Red Spectroscopy
h	Plank Constant
λ	Wavelength
HA- Fe_3O_4	Humic Acid Coated Magnetite
Hcp	Hexagonal Cubic Pack
HS	Humic Substances
K_f	Freundlich Constant
M	Mass Of Adsorbent
MB	Methylene Blue
MNPs	Magnetic Nanoparticles
n	Freundlich Constant
nm	Nano Meter
Nm	Nano Materials

Nps	Nanoparticles
Pzc	Point of Zero Charge
q_e	Adsorbent Capacity at Equilibrium
q_m	Adsorbent Monolayer Capacity
Qt	Adsorbent Capacity at any time t
R_l	Dimensionsless Constant for Langmuir
SEM –EDX	Scanning Electron Microscope Energy Dispersive Spectroscopy
UV-Vis DRS	Ultra Violet Visible Diffuse Reflectance Spectroscopy
XRD	X-Ray Diffractometre

List of figures

List of Tables

1. Introduction

1.1. Background of the Study

Nanomaterials and nanotechnologies attract tremendous attention in recent research due to the wider applications in various fields of study (Aitkin R.J, et al, 2004). It involves the design, synthesis, and application of materials and devices whose size and shape have been engineered at the nanoscale (1 - 100 nm) (Aitkin R.J, et al, 2004). It exploits unique chemical, physical, electrical, and mechanical properties that emerge when matter is structured at the nanoscale (Aitkin R.J, et al, 2004, National Nanotechnology Initiative, 2009).

Nanoparticles (NPs) are important scientific tools that have been used in various biotechnological, pharmacological, technological and waste water treatment technologies (National Nanotechnology Initiative, 2009).They have high surface area to volume ratio and this dominates the contributions made by the small bulk of the material. Several different materials and chemicals have been classified as nanoparticles (NP), such as inorganic metal oxide based NP (titanium dioxide; ZnO; SiO_2, iron oxide, etc.), carbon based NPs (e.g. Fullerenes, carbon nanotubes, carbon black), metal NPs (e.g. nano-scaled (Au, Fe or Ag) and there are still more to be discovered in the future (Perez, S. et al, 2009, Englert, B. C., 2007, Adegboyega N.F,2014). This difference in particle polydispersity between engineered nanoparticles (ENPs) and naturally occurring nanoparticles may be useful for distinguishing between engineered and natural particles (Mauter, M. S.; Elimelech, M., 2008). Today most of the time people use artificial (engineered nanomaterials), which are designed in many commercial products and processes. They can be found in such things as sun block, face paint, sporting clothes, stain-resistant clothing, tires, semiconductor technology, as well as many other everyday items, and are used in medicine for purposes of diagnosis imaging and drug delivery (Satoshi H., Nick S., 2013).

Among different Nanomaterials metal oxide nanoparticles are attractive for a large variety of applications including catalysis, sensors, electronic materials, and environmental remediation due to their stability relative to pure metal NPs (Salabas Lu, 2017). Controlled synthesis of metal oxide nanoparticles is essential for successful application, and solution-phase methods provide a large degree of control over the synthesis products (Salabas Lu, 2017). From the different metal oxide NPs iron oxide NPs (magnetite) are the most attractive and widely studied martial due to the unique combination of high magnetization paramagnetic behavior, super magnetic, availability, non toxic, biocompatible and

magnetic easily separation opens these materials to a very wide range of applications (Salabas Lu, 2017, Hutten, A., et al, 2004, Faraji, M. et al, 2010).

There are different ways of classifying the synthesis routs for nanostructured materials (engineered nanoparticles). One of them is based on the starting state of material (gas, liquid and solid). However, the most popular ways of classifying the synthesis routs is based on how the nanostructures are built, and such approaches leads to two routs ('bottom-up' and 'top-down'). In the bottom-up approach, individual atoms and molecules are brought together or self assembled to form nanostructure materials in at least one dimension (Pokroy B., et al, 2009, Lu, A.H et al, 2007). All techniques that start with liquid and gas as the starting material fall in to this category, Where as in the top-down approach; a microcrystalline material is fragmented to yield a nanocrystalline material. The main disadvantage of the Top-down approach is the imperfection of the surface structure. The nanoparticles produced by the attrition have a relatively broad size distribution and various particle shape or geometry. In addition they may contain significant amount of impurities. All the solid state routs fall in to this category (Lu, A.H et al, 2007).

The synthesis of nanoparticles requires the use of a device or process that fulfills the following conditions: control of particle size, size distribution, shape, crystal structure and composition distribution, improvement of the purity of nanoparticles (lower impurities), control of aggregation stabilization of physical properties, structures and reactants, higher reproducibility , higher mass production, scale-up and lower cost (Aitkin R.J, et al, 2004).

Iron oxide NPs can be synthesized by different chemical methods like co- precipitation, hydrothermal, micro emulsions, sol gel and thermal decomposition method. Magnetite NPs synthesized by cooprcipitation method was found to be the simplest, suitable to modify the surface of NPs by insistu synthesis and most efficient chemical pathway to obtain magnetic nanoparticles (Faraji, M., et al, 2010, Maity D., and Agrawal C., (2007). The magnetite nanoparticles are susceptible to air oxidation and easily aggregated in aqueous system. These properties can be improved by surface modification with different surface coating materials (Griffith J.R., 1981, Tombacz, E, et al, 2006).

The coating of surface materials is protective of the material that serves to make the material properties more attractive, easier to use, control particle size, provide different binding site and can be used for a long time (Tombacz, E, et al, 2006). Different polymeric materials are used for nano material coating but for this study humic acid has been selected because it is biopolymer material contains macromolecules with amino acid, amino sugars, peptides, and aliphatic compounds involved in linkages

between the aromatic groups and many of functional group like carboxylic, phenol and amine. This makes humic acid strongly coated to magnetite by ligand charge reaction and it is confirmed that humic acid adsorbation modifies the surface charge properties of magnetite depending on the amount of adsorbed polyanions (Carlos, L., 2012, Maity D. and Agrawal C., 2007, Etolka tombacz, 2003).

The particle surface can be covered partially or completely with increasing HA concentration, therefore the positive charge of magnetite are neutralized then recharged at the pH lower than point of zero charge (PZC) of oxide surface. The existence of remaining positive charge on the surface and the development of negative particles charge even below PZC were provided electro kinetic measurements. In the presence of trace amount of HA, electrostatic attraction takes place b/n positive and negative charges exist in partially coated magnetite surface. Therefore, modification by coating HA on Fe_3O_4 particle surface enhanced the stability of nano dispersion by preventing their aggregation by electrostatic, steric or combined stabilization layer, increasing the absorption capacity and did not clot in a wide pH range. Humic acid coated magnetite nanoparticles used for removal of cationic pollutant like heavy metals (Etolka tombacz, 2003, Qadri S., et al, 2009). But its application for the removal of cationic organic dye (such as methylene blue) from the aqueous solution was not well studied.

Organic dyes are widely used in various fields and seriously induce water pollution (Huang, S., et al, 2008). Most of the industrial dyes are toxic, carcinogenic, and teratogenic and unfortunately most of them are stable and resistance to photo degradation, biodegradation, oxidizing agents (Ambashta R.D., Sillanpaa M., 2010). From the different forms of dyes methylene blue (MB) is one kind of common industrial dyes, is usually used for dying wood, silk, and cotton. It is harmful to human beings, animals, and plants. So, the treatment of wastewater containing such dye is very important. Adsorption technique becomes one of the preferable choices to purify the waste water containing dyes. It is reported as more economical, simpler and capable of efficiently treating dyes in more concentrated form than other conventional methods (Liu Y, et al, 2007). Moreover, adsorption techniques do not lead to secondary sludge disposal problems. Recently, magnetic loaded adsorbent materials have gained special attention in water purification, due to high separation efficiency, simple manipulation process, kind operation conditions and easy specifically functional modifications (Lead JR, Wilkinson KJ., 2006).

1.2. Statement of the problem

Dyes are one of the most hazardous materials in industrial effluents which can cause severe health problems in human beings, since they exhibit high biotoxicity , potential mutagenic and carcinogenic effects. Therefore, the removal of dye from colored effluents has attracted increasing attention. During the last few decays different methods have been studied extensively to reduce or to remove dyes from waste water due to their toxic effects to humans, animals, plants and the aquatic organisms even at small concentrations. Recently, magnetic loaded adsorbent materials have gained special attention to remove dyes from waste water. But the main problem of this magnetite nano particle was aggregation and oxidation in aqueous solution due to high surface energy, strong magnetic attraction among particles and high van der Waals forces. These aggregation and oxidation of magnetite can be improved by coating with polymeric material such as humic acid. HA have many functional groups that responsible for effective stabilizing agent for the magnetite particles by preventing their aggregation and oxidation. Furthermore, it provides many of binding sites for the removal of cationic dyes. Therefore, in this study humic acid coated magnetite nano particles were synthesized and tested for its effective removal of methylene blue (MB) from aqueous solution.

1.3. Significance of study

This study area can provides important baseline information's about the synthesis of humic acid coated magnetite nanoparticles by co-precipitation method and their application in the removal of organic dyes from aqueous solutions. Ultimately, the result of this research work would be applicable for many of the industry for waste water treatment technology.

1.4. Scope of study

This study has been supported by different types of literatures and a series of laboratory experiments. However, the findings of the research are limited to synthesis and characterization of humic acid coated magnetite nanoparticles by wet chemical method which was co precipitation method. The results were also specific to removal of methylene blue (MB) from aqueous solution by adsorption mechanism.

1.5. Objectives of study

1.5.1. Major objective

The major objective of this research was to synthesis and characterizes bare magnetite and humic acid coated magnetite nanoparticles by co precipitation method for removal of methylene blue dye (MB) from aqueous solution

1.5.2. Specific objectives

The specific objectives of the study were:

- To Synthesize and characterize bare magnetite and HA coated magnetite nanoparticles by Fourier transformed infrared spectroscopy (FTIR), scanning electron microscopy-energy dispersive x-ray spectroscopy (SEM-EDX), and X-Ray Diffracto meter (XRD) and UV-Vis spectroscopy.
- To optimize the dye removal efficiency of bare magnetite and HA-Fe_3O_4NPs by varying of adsorbent dosage, contact time, pH and initial dye concentration.
- To determine the kinetics and isotherms of the adsorption models.

2. Literature Reviews

2.1. Nanoparticles in the natural environment

Nanoparticles have always existed in our environment, from both natural and anthropogenic sources. Nanoparticles in air were traditionally referred to as ultrafine particles, while in soil and water they were colloids, with a slightly different size range (Shi JP., 2001).

In urban atmospheres, diesel and gasoline fueled vehicles and stationary combustion sources have for many years contributed particulate material throughout a wide size range, including NPs, amounting to more than 36% of the total particulate number concentrations (Lead JR.,1997). In addition, there is a natural background of NPs in the atmosphere, although the total concentration is low in comparison to potential releases of manufactured NPs (Lead JR., 1997). In aquatic systems, colloid is the generic term applied to particles in the 1-1000 nm size range. The natural nanomaterials (NM) fraction has been sidentified as being of particular concern because of the changes that occur in this size range, although the most important size range in terms of environmental processes (Guo L, Santschi PH., 2006, Cameron FK., 1915).

In soils, natural NPs include clays, organic matter, iron oxides, and other minerals that play an important role in biogeochemical processes. Soil colloids have been studied for decades in relation to their influence on soil development (pedogenesis) and their effect on soil structural behavior (dispersion and crusting) (Lu, A.H. et al., 2004). Of particular relevance to manufactured NMs, soil colloids and other porous media may facilitate the movement of contaminants in soils and other porous media. The various natural processes causes for the formation of NPs [29].

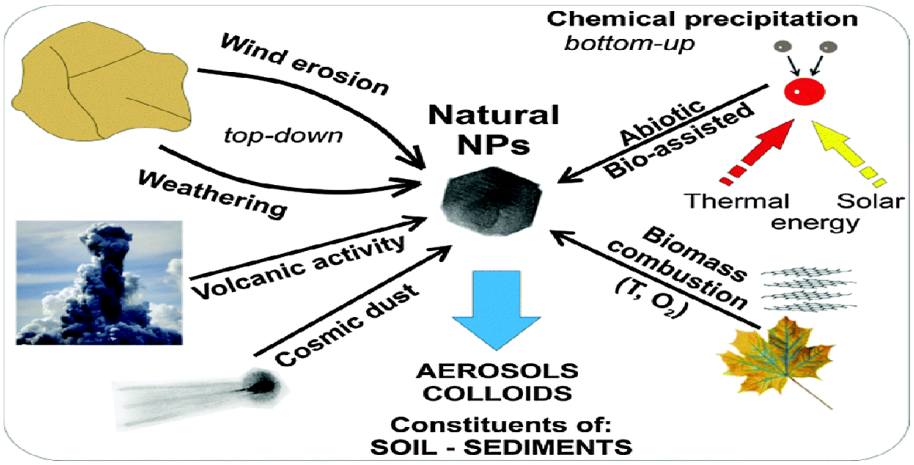

Figure1. Natural processes leading to the formation of nanoparticles in the environment (Natural NPs – natural nanoparticles; T– temperature; O_2– oxygen) (Cameron FK., 1915). .

2.2. Iron based nano materials

Iron based nanoparticles have been studied extensively over the past couple of decades due to their wide range of applications including recording media, environmental remediation and biomedicines **(**Beveridge, J.S. et al., 2011). With increasing interest in their use for the latter applications, there are some critical issues in the nanoparticles that need to be addressed with their in-vivo applications and waste treatment technology. These include a strong magnetic susceptibility, aqueous dispersion, uniform size and shape, biocompatibility and fictionalizations with the desired surface chemistry (Teja, A.S. & Koh, P.Y., 2009).

Iron oxide nanoparticles occur naturally in the earth's crust by various environmental sources such as volcanoes and fires. It exists in many forms in nature (Guo L, Santschi PH., 2006). It mainly exist in oxide forms since , Magnetite (Fe_3O_4), Maghemite (Υ-Fe_2O_3) and Hematite (α-Fe_2O_3) are the most common forms and are stable at room temperature in term of their chemical constitution (Jain T.K., et al, 2005). These oxides are also very important in the field of scientific technology and are therefore the subject of this review.NPs composed of ferromagnetic materials and with size 10–20 nm exhibit an inimitable form of magnetism, i.e., Superparamagnetism. The ferromagnetic materials include elemental metals, alloys, oxides, and other chemical compounds that are magnetized by an external magnetic field. This is an important phenomena normally present only in NP system. Maghemite (γ-Fe_2O_3) is reddish brown in color and it occurs in soil as a weathering product of magnetite. Hematite (α-Fe_2O_3) is the oldest known of the iron oxides and is sometimes referred to as ferric oxide. At ambient condition, these iron oxides are extremely stable and often may occur as the end products of transformation of other iron oxides (Jain T.K., 2005). Iron oxides are usually arranged in close packed lattices in hexagonal (hcp) or cubic (ccp) arrangements, where interstitial sites are partially filled by Fe^{2+}or Fe^{3+}, mostly in octahedral sites, and in a few cases in a tetrahedral geometry (Jain T.K., etal 2005, Beveridge, J.S. et al., 2011). Among those iron oxides magnetite is the most widely studied due to its exhibits the strongest magnetism of all three mentioned iron oxides.

Table 1. Physical and magnetic properties of iron oxide nanoparticles (Jain T.K., etal 2005).

Property	Magnetite	Maghemite	Hematite
Molecular formula	Fe_3O_4	γ Fe_2O_3	α-Fe_2O_3
Lattice parameter (nm)	a = 0.8396	a= 0.8347	a = 0.5034
Crystallographic system	Cubic	Cubic or tetrahedral	Hexagonal
Structural type	Inverse spinel	Defect spinel	Corundum
Type of magnetism	Ferromagnetic or super paramagnetic	Ferromagnetic or super paramagnetic	Weakly ferromagnetic

2.2.1. Magnetite (Fe_3O_4)

Magnetite occurs in nature as magnetic ore, known as lodestone. Magnetite differs from the majority of other iron oxides in that it contains both trivalent and divalent iron ions and also known as black oxide. It has cubic inverse spinal structure with oxygen form a face centered cubic close packing while iron action occupies the interstitial tetrahedral and octahedral sites. Fe (III) cations occupy the tetrahedral sites, while the other half occupies the octahedral sites accompanying with Fe (II) cations (Maeda M., 2006). Iron oxide nanoparticles have one more special property in the form of Superparamagnetism especially with the size ranging from 2 to 20 nm in diameter along with small size and high surface area. It is a form of magnetism especially shown by sufficiently small size nanoparticles in which magnetization can randomly change direction under the influence of temperature and time taken to flip the direction from one stage to another is called as Neil Relaxation time. Hence their magnetization value cannot be measured in the absence of external magnetic field. In the presence of magnetic field they show a good magnetic susceptibility when compare to paramagnets (Jain T.K., et al 2005, Maeda M., 2006) .

Currently magnetite nanoparticles with novel properties and functions have been widely studied in the field of separation technologies due to its cost effective synthesis, easy coating or surface modification and ability to control or manipulating materials on a nanoscale dimensions provide amazing versatility in separation techniques. Apart from these, low toxicity, chemical inertness and biocompatibility of iron oxide nanoparticles show the potential in biomedicines application and highly apposite in adsorption technology for environmental remediation (Ainsworth, C. C., and M. E. Sumner., 1985).

2.2.2. Coatings of Iron Nanoparticles and Its Surface Chemistry

Iron oxides have a completely hydroxy1ated surface. 'This reactive surface makes Fe oxides act as efficient sorbents for anions, cations, and uncharged molecules. Therefore, Fe oxides play a vital role in the transformations of nutrients and pollutants in soils and associated environments (Schwertmann, U., et al, 1989, Ainsworth, C., et al, 1994). The surface of Fe oxides is the region of their interaction with the soil solution, other soi1 solid phases, plant roots, and soil biota (Borggaard, O. K., 1983b). Thus, surface properties such as surface chemical composition and structure, surface electronic properties, surface charge, surface area, surface morphology and surface geometry should be the principal determination of the reactivity of the sorbents and directly govern their behavior in the soil and associated aquatic environment. Some information on the surface area and point of zero charge (PZC) of pure Fe oxides and the influence of adsorption of ligand on the surface chemistry of Fe oxides after they have been formed is available (Xia T, Wang J, et al., 2012, Jain TK, 2008).

According to Wang J, *et al. 2012,* studies Iron oxides with bare surface tend to agglomerate due to strong magnetic attraction among particles, van der Waals forces, and high surface energy. Consequently, the surface coating eliminates the agglomerated iron oxide NPs. High concentration of local Fe ions is also toxic to organisms from Fe dissolution. These can be avoided by coating a shell on the iron oxide NP surface which makes them hydrophilic, compatible to bioenvironments,and functionalized (Hui C, et al., 2011).The appropriate surface coating allows a targetable delivery with particle localization in a specific area and is also considered nontoxic and biocompatible. So far, most work has been carried out to improve the biocompatibility of this material, but regarding the improvement in the quality of magnetic particles, their size distribution, shape, and surface, very few scientific investigations and developments have been carried out. The nature of surface coating of NPs and geometric arrangement not only determines the overall size of the colloid but also plays a significant role in biogenetics and biodistribution of NPs in the body (Petcharoen K, Sirivat A., 2012). For NPs the types of coating or derivatization depends on the application. The synthesis of iron oxide NPs coated with biological molecules, like, gluconic acid, lactobionic acid, silicon oxide, humic acid and polyacrylic acid, through the most effective method of co precipitation as compared to organic solvent heating method (Chen Y., and Aviad T., 1990, Cundy A.B., et al, 2008).

Humic acid (HA): - From physiochemical point of view humic acids are complex aggregate of brown to dark colored amorphous high molecular weight substances, united by general principle of structure, but have some distinctions, which depend on their origin (Stevenson F.J., 1982). They are one of the

most important components of humic substance (HS), help break up clay and compacted soils, assist in transferring micronutrients from soil to plants, enhance water retention, increase seed germination rates, and stimulate the development of micro flora populations in soils. It also slows down water evaporation from soils. This is especially important in soils where clay is present at low concentration or not at all, in arid areas, and in sandy soils without the capability to hold water, provide sites for micro flora to colonize (Ogner G., and Schnitzler M., 1970).

The chemical structure of HAs is very complicated and depends on their source. The main source for humic acid is forest soil, highly weathered soil, compost, black liquaire, peat, lignite and lionardite. From these forests soil and lionardite have high humic acid composition. The elemental composition of different HAs shows that the major elements in their composition are C, H, O, N, and S.) (Frimmel F.H and Christman R.F, 1988).

As shown in the figure 2 humic acid has many functional groups. Some laboratory findings showed that up to 50% of the aliphatic structures in humic acids consist of n-fatty acid esterified to phenolic -OH groups [46]. The remaining aliphatic is made up of more "loosely" held fatty acid and alkane structures. These structures appear to be physically adsorbed onto the humic materials which structurally are not humic components but possibly aliphatic chains joining aromatic rings. The specific functional groups of humic acids are responsible for chelating various compounds in the environment, thereby improving nutrient utilization and preventing metal toxicity in waters, soils, and possibly in plants, animals and humans as well. Humic acids from peats and forest soil show significant levels of phenolic carbons (C6), and methoxy carbons ($-OCH_3$), associated with the presence of lignin-like material when lignin is the starting material of humic acid. The variable molecular composition of humic acids allows a wide range of dissociation constants for the metals that are chelated by humic acids. Different metals are bound to humic acid with varying strength, which means that a particular metal chelate bond modifies the binding stability of the other metal linkages (Frimmel F.H and Christman R.F, 1988, Kim, D.K.,et al, 2001) According to different literature nanoparticles coated by humic acid can increase the application of the material especially in adsorption technology so that it is believed to that humic acid can in increase the dye removal efficiency.

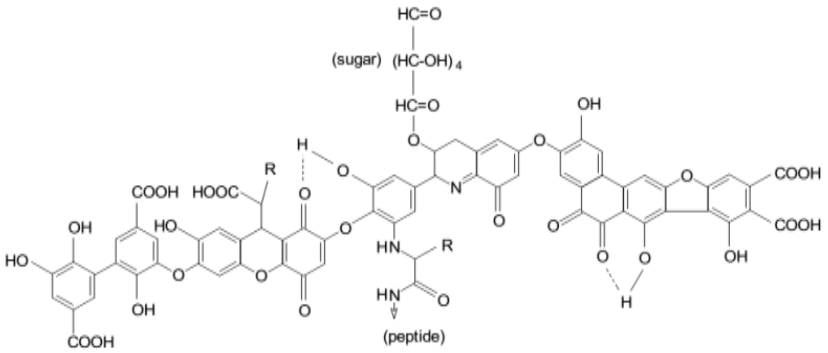

Figure 2 .Model structure of humic acid according to Stevenson (1982); R can be alkyl, aryl or aralkyl.

2.3. Synthesis Method of Magnetic Nano particles

In recent decades, great efforts have been devoted to the synthesis of super paramagnetic iron oxide nanoparticles (SPION) due to their potential applications in several diverse fields. Since the SPION behavior strongly depends on size, surface chemistry and state of aggregation of the particles, preparation methods to produce nanoparticles with unique properties are required. Particularly during the past few years, many publications have described efficient and number of synthetic methods has already been reported in different literatures for the preparation of magnetite nanoparticles like Co-precipitation sol gel, hydrothermal, Thermal decomposition, and Micro emulsion etc.

2.3.1. Co - Precipitation

This method is a facile and convenient way to prepare magnetic nanoparticles. SPIONs can be synthesized by co-precipitation of $Fe^{3+}$and Fe^{2+}aqueous salt solutions by addition of bases under inert atmosphere at room temperature or at elevated temperature. The reaction involves the simultaneous occurrence of nucleation, growth and agglomeration of synthesized nanoparticles**.** Magnetite is usually prepared by an aging stoichiometric mixture (1: 2) of ferrous and ferric salts in aqueous medium. The precipitation of Fe_3O_4 is expected at a pH between 8 and 14. Precipitates are subsequently dried at appropriate temperatures to yield the final powder (Jolivet J. P, Chanéac C. and Tronc E., 2004).

The size and shape of the nanoparticles can be controlled by adjusting pH, $F^{3+}$and Fe^{2+}ratio, ionic strength, temperature and nature of the salts (chlorides, nitrates, sulphates, etc.). Particles with sizes ranging from 5 to 100 nm have been obtained using this method (Laurent S, et al, 2008). This method allows the preparation of large quantities of nanoparticles in a single batch; however, the size distribution is usually not very narrow The addition of chelating organic anions, such as carboxylate ions

(e.g. citric, gluconic, or oleic acid) or polymer surface complexing agents (e.g. humic acid, dextrin, carboxydextran, starch, or polyvinyl alcohol) during the formation of magnetite can help to control the size of the nanoparticles, aggregation and oxidations (LopezPerez, J.A., LopezQuintela, M.A., Mira, J. & Rivas, J., 1997). SPIONs (either Fe_3O_4 or γ-Fe_2O_3) and ferrites are usually prepared in aqueous medium with this approach. .

The magnetite is an amphoteric solid, which can develop charges in the protonation and deprotonation reaction of Fe-OH sites on surface. This process is controlled by the pH and ion strength in aqueous medium. At pH lower than the point of zero charge (PZC) (pH < 7.9) the surface charge is positive, electrostatic interaction between HA and Fe_3O_4 is dominant under acidic conditions.

$$Fe\text{-}OH_2^+ + R\text{-}COO^- \longrightarrow Fe\text{-}OOC\text{-}R + H_2O \quad \text{..... (1)}$$

At above the pH of PZC (pH > 7.9) the surface charge is negative, the coating HA on Fe_3O_4 in alkaline condition, the dominant interaction between HA and Fe_3O_4 is probable a ligand charge reaction with surface hydroxyl (Carlos, L., et al, 2012).

$$Fe\text{-}OH + R\text{-}COO^- \longrightarrow Fe\text{-}OOC\text{-}R + OH^- \quad \text{..... (2)}$$

2.3.2. The Micro emulsion

Micro emulsions are isotropic, thermodynamically stable single-phase colloidal dispersions which consist of spherical aqueous nano droplets called micelles surrounded by surfactant molecules. Micro emulsion systems comprise three components: water, oil and an amphiphilic molecule, called a surfactant. The surfactant molecule, which could be cationic (cetyltrimethylammonium bromide), anionic, (bis (2-ethylhexyl) sulfosuccinate), and nonionic, Synperonic® 6/10), lowers the interfacial tension between the water and oil, resulting in the formation of a transparent solution (Vidal-Vidal, J., Rivas, J. & Lopez-Quintela, M.A., 2006).

This method is similar to the co-precipitation method but instead of using an aqueous solution, a micro emulsion solution is used. The water or oil nano droplets which contain reagents as a nanoreactors undergo rapid coalescence, a precipitation reaction followed by an aggregation process. These nanoreactors act as a confined environment for particle growth, which reduce the average size of the particles during the collision and aggregation process (Faraji, M., Yamani, Y. & Rezaee, M., 2010). However this method may require a large amount of solvent to prepare an appreciable amount of particles, lower product, costy and high carbon content end product.

2.3.3. Hydrothermal

Under hydrothermal synthesis, a wide range of nanoparticles can be formed. These reactions are performed in an aqueous medium in autoclaves or reactors under high pressure and temperature. The hydrothermal method has been reported as being environmentally friendly a versatile since it does not involve the use of any organic solvent (Lian, S.Y. et al. 2004). Thus, it has been widely studied for the preparation of metal oxide nanoparticles. Reduction of metal ions under hydrothermal conditions is being utilized in the preparation of iron oxide nanoparticles, using metal salts, polyethylene glycol and sodium acetate (Schwarzer H.C and Peukert W., 2004).

The slow reaction kinetics at any given temperature is one of the limitations of this method; in addition, the engineering of nanoparticles surfaces cannot be accomplished in situ therefore additional post-processing steps are required, Prior knowledge on solubility of starting materials is required and Hydrothermal slurries are potentially corrosive and accidental explosion of the high pressure vessel cannot be ruled out (C. J. Brinker, G. W. Scherer., 1990).

2.3.4. Sol-Gel Process

Sol-gel is the multi step process involving chemical and physical processes associated with hydrolysis, polymerization, gelatlon, condensation, drying and densification (Schwertmann, U., Gasser U., and Sticher H., 1989). This process generally starts with the mixing of metal alkoxides or salts in water or in a suitable solvent (usually an alcohol) at ambient or slightly elevated temperatures (C. J. Brinker, G. W. Scherer., 1990). In sol gel process, controlling the pH of starting solution is very much important to avoid the precipitation as well as to form the homogenous gel, which can achieved by the addition of base or acidic solutions . Apart from the above, organic compounds with hydrophilic functional groups (hydroxides or carboxylate) in small molecules such as citric acid, succinic acid, oxalic acid, tartaric acid, acrylic acid, etc and polymers like polyacrylic acid (PAA) and polyvinyl pynolidone (PVP) can be used with metal ion sources to form the sol as well as control the particle size and uniformity of the products (Fu L.J., et al, 2005). Chelation of metal ions by carboxylic acid groups lead to a homogeneous distribution of the constituent ions in the obtained gel (Li, Y., Afzaal, M., & O'Brien, P., 2006). The gel intermediate is further heated between 150 "C and 300 "C to eliminate volatile organic components, excess water, etc., which results the dried intermediate powders. Single phase nanocrystalline metal oxides are obtained after calcining of dried gel powder at 400-800 "C depends on the precursor chemical nature ((Li, Y., Afzaal, M., & O'Brien, P., 2006).

Main process of sol –gel are:-

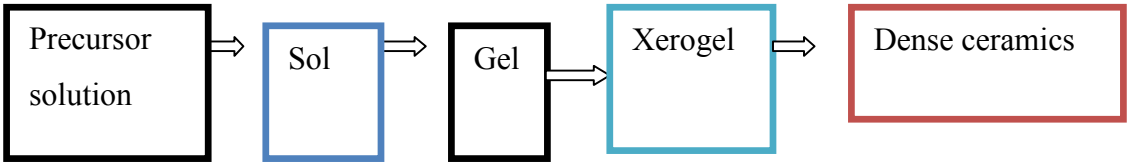

Figure 3 Sol-gel process flow chart

However this method disadvantages like raw materials for process is expensive (in the case of metal alkoxides) compared to mineral based metal ion sources ,Products would contain high carbon content when organic reagents are used in preparative steps and this would inhibits densification during sintering and Since several steps are involved, close monitoring of the process is needed.

2.3.5. Thermal Decomposition

Another method of preparing quality semiconductor nanocrystals and magnetic nanoparticles with a high level of monodispersity and tunable size is by the use of thermal decomposition. This is achieved when oregano metallic precursors such as metal acetylacetonates, metal cupferronates [FeX Cupx] where (Cup = N-nitosophenylhydoxyl amine) or carbonyls (iron pentacarbonyl) are heated in high-boiling organic solvents and a surfactant such as oleic acid or hexadecylamine (Hyeon, T., et al, 2001, Park, J. et al. 2004).

Metal oxide magnetic nanoparticles including iron oxide nanoparticles can also be prepared by the thermal decomposition method. To date, two different approaches have been used for this purpose in order to avoid the use of highly toxic compounds such as metal carbonyls. Hyeon et al. in their procedure used cheap and environmentally friendly $FeCl_3$ and sodium oleate. The first step consists of iron oleate, or stereate precursors that decompose in a second step by slowly heating the mixture to 320 ^{o}C to form the desired nanoparticles. The size and morphology of the magnetic nanoparticles can be affected by factors like the ratio of the starting reagents, for instance organo metallic compounds, solvents and surfactants (Zhang J.Z., et al, 2003). The reaction time, reaction temperature and aging time are also critical. Even though thermal decomposition seems well suited for the preparation of controlled size and high crystalline nanoparticles, one of the drawbacks of this method is the uncertainty of whether the prepared nanoparticles can be suspended in aqueous media, which limits the extent of their applications in biological and environmental fields. Furthermore, this method usually leads to complicated processes or requires relatively high temperature and inert atmosphere, thereby making synthesis time-consuming and expensive (Zhang J.Z., et al, 2003).

Among the above described methods, co-precipitation and micro emulsion methods have shown success, and are widely utilized in the synthesis of super paramagnetic iron oxide nanoparticles for biomedical and environmental applications. Normally, they are preferred due to their facile and convenient preparation approach, low production cost, as well as reproducibility. Moreover, the working window for these two methods, especially co precipitation, is quite large; thus, it promotes the surface chemistry modification of the nanoparticles during the synthesis (in situ) or after synthesis. Another advantage of cooprcipitation and micro emulsion methods is that the reaction temperature and time preparation are much lower than in the other methods.

2.4. Characterization of Magnetic Nanoparticles

Structural characterization is essential for nanomaterials research. Since the nanostructures are usually too small to be visualized with conventional optical microscopes, it is important to use appropriate tools which adequately characterize their structure and surface in detail at the molecular or atomic level. This is important not only for understanding their fundamental properties but also for exploring their functional and technical performance in technological applications. There are several experimental techniques that can be used to characterize structural and surface properties of nanomaterials either directly or indirectly, e.g. X- Ray diffractometre (XRD), Scanning Electron Microscope (SEM), Transmission Electron Microscope (TEM), Forier Transfer Infrared Spectroscopy (FTIR) , Ultra Violet Visible spectroscopy (UV – Vis) and others used to characterize nano materials (Takafuji, M., et al, 2004, Boutonnet, M., et al, 2008, .

2.4.1. X-Ray Diffractometre (XRD)

XRD is a powerful and routine technique for determining the crystal structure of crystalline materials (Murray C.B., 1995, Barr T.L., Modern ESCA., 2008). Consider two parallel monochromatic X-ray beams with the wave length of λ falling on the successive planes of the crystal at an angle of2θ. Constructive interference of the reflected rays from two successive planes occurs, only the path difference between the two rays fulfils the Bragg's condition,

$$n\lambda = 2d\ \text{sine}\theta \qquad (3)$$

Where n is integer and d is aninter planar distance. By examining the diffraction pattern, one can identify the crystalline phase of the material. Small angle scattering is useful for evaluating the average interparticle distance while wide-angle diffraction is useful for refining the atomic structure of nanoclusters. The widths of the diffraction lines are closely related to the size, size distribution, defects

and strain in nanocrystals. As the size of the nanocrystals decreases, the line width is broadened due to loss of long range order relative to the bulk. This XRD line width can be used to estimate the size of the particle via the Debye– Scherer formula.

$$D = \frac{k}{\beta \cos \theta} \lambda \quad \text{...} \quad (4)$$

Where D is the nanocrystals diameter, k, is Scherer constant, λ is the wavelength of light, β is the full width half at maximum (FWHM) of the peak in radians, and θ is the Bragg angle

2.4.2. Scanning Electron Microscope –Energy Dispersive X-ray spectroscopy (SEM -EDX)

SEM is a powerful and popular technique for imaging the surfaces of almost any material with a resolution down to about 1 nm (Hanada N., et al, 2008). The image resolution offered by SEM depends not only on the property of the electron probe, but also on the interaction of the electron probe with the specimen. The interaction of an incident electron beam with the Specimen produces secondary electrons, with energies typically smaller than 50 eV, the emission efficiency of which sensitively depends on surface geometry, surface chemical characteristics and bulk chemical composition (Liu Z.L., et al, 2008). SEM can thus provide information about the surface topology, morphology and chemical composition. The high resolution capability afforded by SEM makes it convenient for probing nanomaterials of which the structural features on the nanoscale are critical to their properties and functionalities.

Principle:-A typical scanning electron microscope starting from the electron source; a stream of monochromatic electrons generated by an electron gun is condensed by the first condenser lens to both form the beam and limit the amount of current, as well as, in conjunction with the condenser aperture, to eliminate the high-angle electrons from the beam. The second condenser lens focuses the electrons into a thin, tight, coherent beam and an objective aperture is used to further eliminate high-angle electrons from the beam. A set of coils is used to scan the beam in a grid fashion. The objective lens focuses the scanning beam onto the specimen desired, one point at a time. Interaction between the electron beam and the sample generates back scattered electrons (BSE), X-ray, secondary electrons (SE), and Auger electrons in a thick or bulk sample. These various electrons are detected and the signal detected contains information about the specimen under investigation. BSE is more sensitive to heavier elements than SE. The X-ray radiation can be detected in a technique called energy dispersive X-ray (EDX) spectroscopy that can be used to identify specific elements (Liu Z.L., Deng J.C., et al, 2008, Brydson R, Brown A., 2008). Nevertheless, SEM can yield valuable information regarding the purity of a nanoparticles sample

as well as an insight on their degree of aggregation. Moreover, when nanoparticles are part of secondary and tertiary nanostructures, SEM becomes a valuable tool to assess their location. The location of the metal nanoparticles over the support is evident. Furthermore, the SEM micrograph clearly reveals the high degree of dispersion and uniformity of these metallic nanoparticles over the substrate.

2.4.3. Transmission Electron Microscope (TEM)

The development made in TEM has enabled the direct imaging of atomic structures in solids and surfaces. Nanometer sized particles are commonly present in many different types of materials and the use of TEM allows for gathering information about particle size, shape, and any surface layers or adsorbate (Howe JM, et l, 2008). More recently, changes in nanoparticles structure as a result of interactions with gas-, liquid-, or solid-phase substrates can now be monitored by this technique (Silverstein RM and Webster FX, Ed.v, 2002).

TEM is a high spatial resolution structural and chemical characterization tool (Silverstein RM and Webster FX, Ed.v, 2002). A modern TEM has the capability to directly image atoms in crystalline specimens at resolutions close to 0.1 nm, smaller than interatomic distance. An electron beam can also be focused to a diameter smaller than ~ 0.3 nm, allowing quantitative chemical analysis from single nanocrystals. This type of analysis is extremely important for characterizing materials at a length scale from atoms to hundreds of nanometers. TEM can be used to characterize nanomaterials to gain information about particle size, Shape, crystallinity, and interparticle interaction (Hanada N., et al 2008)

Principle: - A stream of monochromatic electrons produced by an electron gun is focused into a small, thin, coherent beam by two condenser lenses. The electron beam is restricted by the condenser aperture to remove high angle electrons before it reaches the specimen. It is important in this case that the specimen is thin enough to allow some electrons to transmit through the sample. Interaction between the electron beam and specimen generates elastically and in elastically scattered electrons, along with some un scattered electrons, in the forward direction after the sample has been detected. The detected signal contains information about the sample. The detection involves several lenses to focus the electrons to be detected before they reach the detection phosphor screen. Optional objective and selected area metal aperture that can be used to restrict the beam, with the objective aperture enhancing contrast by blocking out high-angle diffracted electrons and the selected area aperture enabling the user to examine the periodic diffraction of electrons by ordered arrangements of atoms in the sample examined.

However, this method have some limitations, image overlap is a typical problem during observation ,very expensive , Moreover, nanoparticles can be susceptible to damage under the electron beam irradiation conditions normally used for high-resolution imaging.

2.4.4. Forier Transfer Infrared spectroscopy (FTIR)

The infrared spectra are recorded on Fourier Transform Spectrometer in the mid–infrared region (MIR) within the range (400-4000 cm^{-1}). It is a powerful technique for identifying the structural coordination (types of chemical bonds) in the substances such as solids, liquids and gases. It is based on the interaction of IR radiation with the substance and the nature of interaction, which reveal the properties of the substance.

Due to the complex interaction of atoms within the molecule, IR absorption of the functional groups may vary over a wide range. However, it has been found that many functional groups give characteristic IR absorption at specific narrow frequency range. Multiple functional groups may absorb at one particular frequency range but a functional group often gives rise to several characteristic absorptions. Stretching & bending vibrations are varied after formulation can be observed. Thus, the spectral interpretations should not be confined to one or two bands only actually the whole spectrum should be examined (Perkampus H.H., 1994).

Principle: - When infrared radiation passes through a sample (solid, liquid or gas), certain frequencies of the radiation are absorbed by the molecules of the substance leading to the molecular vibrations. The frequencies of absorbed radiation are unique for each molecule which provides the characteristics of a substance. Since, the strength of the absorption is proportional to the concentration.

2.4.5. Ultra Violet Visible Diffuse Reflectance Spectroscopy (UV-Vis DRS)

Many molecules absorb ultraviolet (UV) or visible light. The absorption of UV or visible radiation is can use by the excitation of outer electrons, from their ground state to an excited state. The Bouguer-Lambert-Beer law forms the mathematical physical basis for the light absorption measurements on gas and in solution. According to this law, absorbance is directly proportional to the path length l, and the concentration of the absorbing substance, c, and can be expressed as $A = \varepsilon bc$, where ε is a constant of proportionality, called the absorptivity. In addition, absorption strongly depends on the types of samples, and the environment of the sample. For instance, molecules absorb radiation of various wavelengths depending on the structural groups present within the molecules, and show a number of absorption bands in the absorption spectrum. The solvent in which the absorbing species is dissolved also has an

effect on the spectrum of the species. Moreover, the size of the particle is also important. If the size of the particle d>>λ, light interacts with the samples instead of absorption, with parts of the light scattered and reflected (Rajabia A.,et tal, 2016).

The band gap energy of nanoparticles can be calculated by the following formula:-

$$\text{Band gap energy } (E_g) = \frac{hc}{\lambda} \text{ ……………………………… (5)}$$

Where h is Planks constant = 6.626 x 10^{-34} Joules sec c is Speed of light = 3.0 x 10^{8} meter/sec λ is Wave length.

When dealing with solid samples light penetrates into the sample undergoes numerous reflections, refractions and diffraction and emerges finally diffusely at the surface. The Bouguer-Lambert-Beer law cannot handle solid samples, which is based on the assumption that the light intensity is not lost by scattering and reflection processes. Diffuse reflectance measurements are usually analyzed on the basis of the Kubelka Munk equation:

$$F(R\infty) = \frac{K}{S}(1-R)^2\backslash 2R\text{……………………..(6)}$$

Where k and s are absorption and scattering coefficients respectively, and R is the reflectance at the front face. F (R∞) is termed the Kubelka Munk function and is proportional to the concentration of the adsorbate molecules. From the onset of the plot of Kubelka Munk function vs wavelength of photo energy, the band gap energy of a semiconductor can be easily calculated. However, to measure a diffuse reflectance spectrum, the diffusely reflected light must be collected with an integrated sphere, avoiding secularly reflected light, and using a reference standard (BaSO4 or white standards.

2.5. Application of Magnetic Nano sorbent and other adsorbents on dye removal

The common adsorbents primarily include activated carbons, highly porous materials, biomass and polymeric materials, etc. Although widely applied in research and practical applications, these materials still have limitations. Activated carbon has been engineered for optimal adsorption of the contaminants found in dye house effluents: large, negatively charged or polar molecules of dyes (Shiva Dehghan Abkenar, (2016). Activated carbon is the most widely used sorbent, and it has excellent sorption properties for a considerable number of synthetic dyes. However, the preparation of carbon sorbents is generally energy intensive, making commercially available products relatively expensive. Because a large amount of carbon sorbent is needed to remove the dye from a large volume of effluent, high cost

can hinder its application (Baban, A., et al, 2010). Activated carbons and porous materials have the disadvantages such as difficulty in collection due to small particle size, high regeneration temperatures (e.g., 800-850 °C for activated carbon) and low separation efficiency caused by the co adsorption of water (Baban, A., et al, 2010). Hence, instead of activated carbon, alternative low-cost, novel locally available adsorbents are currently used for removal of textile dye effluents from aqueous solutions. Sepiolite, zeolite , waste metal hydroxide sludge, smectite, bentonite , Sorrel's cement , modified mesoporous silica ,orange peel, polymethyl acryl ate grafted chitosan, magnetic alginate beads and modified magnetic nanoparticles are some adsorbents used in this respect (Shiva Dehghan Abkenar, 2016). The traditional adsorbents have some disadvantages such as relatively limited pollutant removal capacity and poor separation ability as compare to nano adsorbent (Shiva Dehghan Abkenar, 2016).

More recently, magnetic porous materials were demonstrated to realize a fast separation of organic chemicals from water by applying an appropriate external magnetic field (Baban, A., et al, 2010). In fact, the application of magnetic particle technology to solve environmental problems has received considerable attention in recent years. The surface chemistry of coated magnetite nanoparticles develop both negatively charged surface arising from coating material and former positively charged surface at magnetite NPs. Magnetic nanoparticles (MNPs) are a new class of nanoadsorbent which not only possess quite good performance owing to high efficient specific surface area and absence of internal diffusion resistance compared to the traditional adsorbents, furthermore can be recovered rapidly by an external magnetic field. Nanoparticles possessing magnetic properties offer great advantages in that they can provide selective attachment to a functional molecule, confer magnetic properties to the target, and allow manipulation and transportation to a desired location through the control of a magnetic field produced by an electromagnet or permanent magnet (Chen Y., and Aviad T., 1990, Baban, A., et al, 2010).

The adsorption capacity for metal ions with the complexes of HA and iron oxides was reported to be larger than that with the respective iron oxides and HA alone because humic acid coated magnetite nanoparticles has different binding site that arise from the coating material and the former positive charge around the NPs where as non coated magnetite NPs due to aggregation form clusters which has small surface area to volume ratio which limits the removal efficiency (Schwarzer H.C and Peukert W., 2004). HA have also limitations in regeneration of materials, processing time, material preparation, and operating conditions in real time and these need further investigation. In this study, a novel low-cost magnetic sorbent material prepared by coating Fe_3O_4 magnetic nanoparticles with was developed for the removal of organic dyes from aqueous solutions (Börnick, H. & Schmidt, T.C., 2006).

The polluting effects of dyes against aquatic environment can be also the result of toxic effects due to their long time presence in environment (i.e. half-life time of several years), accumulation in sediments but especially in fishes or other aquatic life forms, decomposition of pollutants in carcinogenic or mutagenic compounds but also low aerobic biodegradability. Due to their synthetic nature and structure mainly aromatic, the most of dyes are non-biodegradable, having carcinogenic action or causing allergies, dermatitis, skin irritation or different tissular changes. Moreover, various Azo dyes, mainly aromatic compounds, show both acute and chronic toxicity. High potential health risk is caused by adsorption of Azo dyes and their breakdown products (toxic amines) through the gastrointestinal tract, skin, lungs, and also formation of hemoglobin adducts and disturbance of blood formation[80]. Methylene blue (MB) is one kind of common industrial dyes is usually used for dying wood, silk, and cotton. It is harmful to human beings, animals, and plants. So, the treatment of wastewater containing such dye is very important (Börnick, H. & Schmidt, T.C., 2006).

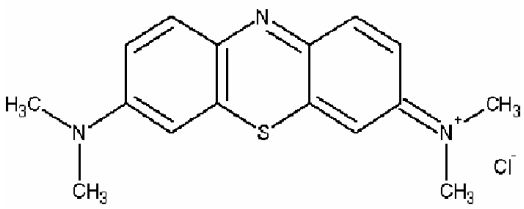

Figure 4 Structure of methylene blue dye (MB)

Various treatment method that have been used to remove dyes from wastewater such as physical (adsorption, irradiation and membrane process), chemical (oxidative process, coronation, ionic exchange, electro coagulation and coagulation-flocculation) and biological (aerobic and anaerobic) treatment .among the described methods of dye removal techniques adsorption is most common and efficient technique to remove dyes (Illes E., and Tombacz E., 2005, Illes E., and Tombacz E., 2006, Ardejani F., et al, 2007, Sajab, M.S.**,** et al, 2013)

2.6. Mechanism of Methylene Blue (MB) removal by magnetic adsorbent.

A separation where in certain fluid elements are transferred to solid surface of the adsorbents is known as adsorption. Transfer of molecules from bulk solution to solid surface occurs based on concentration gradient. Adsorption techniques are used as high quality treatment processes for the removal of dissolved organic pollutants, such as dyes, from industrial wastewater (Kurniawan, T. A. and Lo, W.H.,

2009). Dyes represent one of the problematic groups; they are emitted into wastewater from various industrial branches, mainly from the dye manufacturing and textile finishing and also from food coloring, cosmetics, and paper and carpet industries. It is well known that the dye effluents from dyestuff manufacturing and textile industries may exhibit toxic effects on microbial populations and can be toxic and/or carcinogenic to mammalian animal. Most dyes used in textile industries are stable to light and are not biologically degradable. Furthermore, they are resistant to aerobic digestion (Anjaneyulu, Y., 2005). The dye adsorbed on modified magnetite NPs by electrostatic attraction and $\pi to\ \pi$ interaction. Electro statically results from the interaction between positively charged of dye and negatively charged adsorbent. MB is a kind of cationic dye which can be adsorbed easily by electrostatic forces on negatively charged surfaces of multi walled carbon nanotubes coated magnetite NPs. MB is also an ideally planar molecule and therefore can be easily absorbed by multi walled carbon nanotubes stacking interactions between the aromatic backbone of the dye and hexagonal skeleton of coating materials.

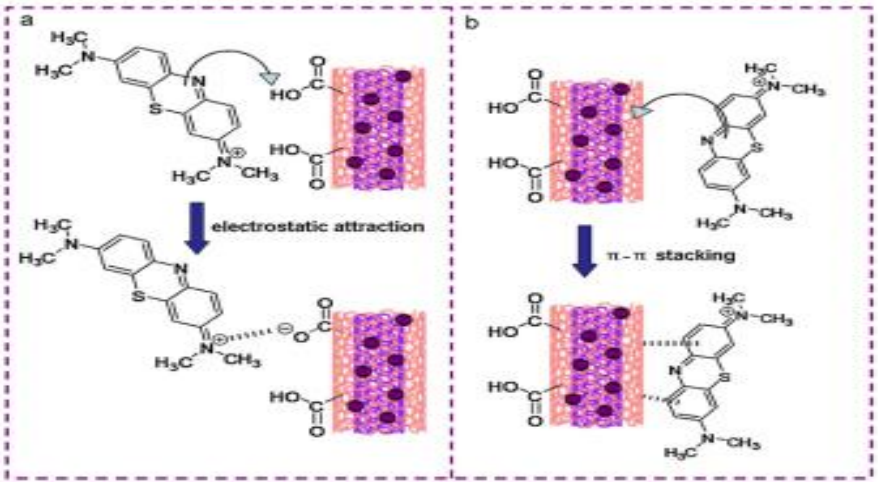

Figure 5.Schematic illustration of the possible interaction between multi walled carbon nanotubes modified Fe_3O_4 and MB: (a) electrostatic attraction and (b) $\boldsymbol{\pi - \pi}$ stacking ((Kurniawan, T. A. and Lo, W.H., 2009).

2.7. Adsorption Process

Decolorization by physical treatment is a result of two mechanisms: adsorption and ion exchange. One of the most effective and proven treatment with potential application in wastewater treatment is adsorption. This process consists in the transfer of soluble organic dyes (solutes) from wastewater to the surface of solid, highly porous, particles (the adsorbent). The adsorbent has a finite capacity for each

compound to be removed, and when is 'spent' must be replaced by fresh material (the 'spent' adsorbent must be either regenerated or incinerated) (Birch, R.R., etal 1989).

Adsorption is an economically feasible process for dyes removal or decolorization of textile effluents being the result of two mechanisms: adsorption and ion exchange. The principal influencing factors in dye adsorption are: dye/adsorbent interaction, adsorbent surface area, particle size, temperature, pH, and contact time. Adsorbents which contain amino nitrogen tend to have a significantly larger adsorption capacity in acid dyes (Aly, Osman, et al 1987). The adsorption amount (qe, $mmolg^{-1}$) of the molecules at the equilibrium step was determined according to the following equation**:**

$$qe = \mathbf{V}\frac{\mathbf{Co-Ce}}{\mathbf{M}} \quad \text{.....} \qquad (7)$$

Where V is the solution volume (mL); M is the mass of adsorbents (g); and Co and Ce are the initial and equilibrium adsorbate concentrations, respectively. The removal efficiency of pollutants by a certain adsorbent can be calculated as:

$$\% \text{ Removal} = \frac{Co-Ce}{Co} X100 \text{.....} (8)$$

2.7.1. Adsorption isotherms and models

An adsorption isotherm is the presentation of the amount of solute adsorbed per unit weight of adsorbent as a function of the equilibrium concentration in the bulk solution at constant temperature. The mechanism of dye removal was studied by isotherm models. The relation between the mass of the dye adsorbed at a particular temperature, the pH, particle size and liquid phase of the dye concentration is discussed by the adsorption isotherms. Langmuir and Freundlich adsorption isotherms are commonly used for the description of adsorption data (Anjaneyulu, Y., et al, 2005).

The **Langmuir** adsorption model explains adsorption by assuming an adsorbate behaves as an ideal gas at isothermal conditions. He hypothesized that a given surface has a certain number of equivalent sites to which a species can "stick", either by physisorption or chemisorption. The Langmuir equation is expressed as:

$$C_e/q_e = 1/ bq_m + C_e/q_m \text{ ..... } (9)$$

Where Ce is the equilibrium concentration of solute (mmol L^{-1}), qe is the amount of solute adsorbed per unit weight of adsorbent (mmol g^{-1} of adsorbate), qm is the adsorption capacity (mmol g^{-1}), or monolayer capacity, and b is a constant (L $mmol^{-1}$) (Anjaneyulu, Y., et al, 2005).

The Freundlich isotherm describes heterogeneous surface adsorption. The energy distribution for adsorptive sites in Freundlich isotherm follows an exponential type function which is close to the real situation. The rate of adsorption/desorption varies with the strength of the energy at the adsorptive sites.

The Freundlich equation is expressed as:

$$\text{Log } q_e = \log k_f + (\log C_e)/n \quad \text{(10)}$$

Where K_f and n are empirical constants incorporating all parameters affecting the adsorption process such as, sorption capacity and sorption intensity respectively (Ai L.H., Zhou Y., Jiang J., 2011).

2.7.2. Adsorption Kinetics

The study of adsorption kinetics describes the solute uptake rate and evidently this rate controls the residence time of adsorbate uptake at the Solid Solution interface. This procedure is similar to that of batch equilibrium studies. The difference is that the absorbent adsorbate solution is taken at preset time intervals and the concentration of the solution is measured (Wang H., et al., 2007). The amount of adsorption at time t, qt (mg/g), describes as :

$$q_t = ((C_o - C_t) /W) \times V \quad \text{(11)}$$

Where C_o and C_t (mg/L) are the liquid-phase concentrations of adsorb ate at initial and at any time t, respectively. V is the volume of the solution and W is the mass of adsorbent used. The adsorption kinetics of dye on adsorbent is investigated using pseudo-first order model and pseudo-second-order model.

2.7.2.1. Pseudo-first-order kinetic model

The pseudo-first-order kinetic model equation is generally expressed in equation 12 [90]:

$$\ln (q_e - q_t) = \ln qe - k_1 t \quad \text{(12)}$$

Where qe is the amount of adsorbate adsorbed at equilibrium, (mg/g), qt is the amount of solute adsorb per unit weight of adsorbent at time, (mg/g), k_1 is the rate constant of pseudo-first order sorption (1/h). A plot of ln (q_e-q_t) versus t gives a straight line with slope of k_1 and intercept of lnqe (Wang H., 2007).

2.7.2.1. Pseudo-second-order kinetic model

In this model, the rate-limiting step is the surface adsorption that involves chemisorption, where the removal from a solution is due to physicochemical interactions between the two phases.

The pseudo-second-order equation can be expressed as :

$$t/q_t = 1/k_2 qe^2 + t/q_e \quad \ldots\ldots (13)$$

Where K_2 [$gmg^{-1}min^{-1}$] is the rate constant of the pseudo second order adsorption, q_e is the amount of dye adsorbed on the adsorbent at equilibrium [mg/g], and q_t is the amount of dye adsorbed on the adsorbent at any time, t [mg/g]. The plot of t/q_t Vs t should give a linear relationship from which qe and K_2 can be determined from the slope and intercept of the plot respectively (Hu C.H, et al, 2009).

2.7.3. Factors affecting the dye removal efficiency

The major factors that can affect the removal efficiency of dyes are, PH, adsorbent dosage and initial concentration on dye concentration and contact time (Ai L.H., Zhou Y., Jiang J., 2011).

Effect of pH: - pH of solution affects adsorption process of dye molecules by affecting both aqueous chemistry and surface binding-sites of the adsorbent. Hu C.H., et al, 2009 observed an increase in the rate of the adsorption of malachite green dye with an increase in pH. The electrical charges on adsorbent materials are known to depend on pH, which is related to the ionization of the polar functional groups on the adsorbent surface. Many researchers have reported that the pH of the basic dye, MB solution, could significantly influence adsorption process (Garg V.K, Kumar R, Gupta R., 2004).

At low pH values, the number of negatively charged adsorbent sites decreased and the number of positively charged sites increased, which did not favor the adsorption of positively charged dye cations like methylene blue due to electrostatic repulsion. In addition, lower adsorption of methylene blue at acidic pH might be due to the presence of excess H^+ ions competing with MB cations for the available adsorption sites which reduce the adsorbed amount. Increasing the pH values will lead to deprotonation of the acid sites on adsorbent surface and the surface becoming negatively charged with high attractive properties.

This leads to increase in the surface diffusion of the dye molecules due to high the electrostatic interactions between MB and adsorbent. This is because of MB is basic in nature and it releases colored dye cations in the solution. Hence, many attempts have been taken to investigate the effect of pH in the removal of pollutants in the west water.

Effect of adsorbent dosage: Adsorbent dosage is a very important parameter in the determination of adsorption capacity**.** According to different researchers and scholars studies (Indira T.K, Lakshmi P.K., 2010, Wei Y., et al, 2012) as the adsorbent dosage increases, the surface area of the adsorbent is

increased as result removal efficiencies of pollutants by the adsorbent increase. Hence, more adsorption sites are available to absorb MB from aqueous solution. Therefore, the equilibrium time will be shorter at higher adsorbent dosage (Wei Y., et al, 2012).

Effect of initial concentration dye:-The effect of MB initial concentration on dye concentration removal is carried out at fixed adsorbent dosage. According Indira T.K., et al, 2010 studies the removal efficiency of MB decreases by a given adsorbent as concentration of dye increases. However, the actual amount of dyes adsorbed per unit mass of adsorbent increased with initial dye concentration ((Indira T.K, Lakshmi P.K., 2010, Wei Y., et al, 2012).

Effect of contact time: -According Indira T.K.,et al, 2010, the contact time between adsorbate and adsorbent is one of the most important design parameters that affect the performance of adsorption processes. The contact time required to achieve equilibrium and complete adsorption for dye. Most of the researchers and scholars reviewed that increasing contact time can increase adsorption efficiency until reach to equilibrium time or occupied the active site of the adsorbent (Indira T.K, et al 2010).

3. Materials and Methods

3.1. Chemicals and Reagents

Chemicals and reagents used for this research work were:- Hydrochloric acid (Riedel dehaen,Germeny,37 % HCl), distilled water, Ferric chloride hexahydrate ($FeCl_3.6H_2O$,Sigma aldria 99% purity) and Ferrous sulphate hepta hydrate ($FeSO_4.7H_2O$, Sigma aldria ,99% purity), 25% ammonium hydroxide, Sodium hydroxide(NaOH) , Methylene blue, ultra pure ethanol (99.99 % purity) ,Sodium chloride (NaCl) and Humic acid (sigma aldria chemie gmbh).All chemicals were used without further purification.

3.2. Apparatus and Instruments

The apparatus and instruments used for this research work were :-Oven , Shaker (SK300), UV-Vis spectroscopy (T80+- PG instruments), UV-Vis Diffuse reflectance spectroscopy(UV-Vis DRS, Elico SL-150 spectrophotometer), X–ray diffractometre (Shimadzu, XRD-7000S South Korea), scanning electron microscope-energy dispersive x-ray spectroscopy (SEM- EDX), Carl Zeiss Model: Neon-40, FESEM/FIB), Fourier transfer infrared spectroscopy (FTIR Perkin Elmer's spectrophotometer) , mortal , electronic balance (ESJ200-4), beaker, PH meter (HANA Instruments-210),universal indicator, round bottle flask ,ceramic crucible, conical flask, measuring cylinder, what man filter paper, Buckner funnel, glass bottle, magnetic stirrer, bare magnate, and centrifuge.

3. 3. Synthesis of Fe_3O_4 and HA/Fe_3O_4 NPs

Humic acid coated magnetite nanoparticles was synthesized by co-precipitation method using its precursor, ferric chloride hexa hydrate ($FeCl_3$ $.6H_2O$), ferrous sulphate heptahydrate ($FeSO_4.7H_2O$), ammonium hydroxide and humic acid as coating agent. The binding of HA on Fe_3O_4 was essentially altering the surface properties, stability of colloidal magnetite, controlling the particle size, pressing strength and stability of the magnetic properties of penetration and effectively preventing their aggregation.

Fe_3O_4 NPs was synthesized in Adama science and technology research laboratory of applied chemistry department by the Co-Precipitation method (Maity, D.; Agrawal, D. C., 2007, Soerja Koesnarpadi, et al 2017). Firstly, the mass of iron salts, $FeCl_3.6H_2O$ (6 g) and $FeSO_4.7H_2O$ (4 g) was measured using electronic balance in the stoichiometric ratio of (3:2) and was dissolved in 100 mL water in conical flask and heated to 9^0C for three minute. Secondly 15 mL of 25% NH_4OH was added as precipitating agent gradually followed by stirring using magnetic stirrer until a black powder was formed in the solution.

Then the mixtures was aged at 90^0C for 30 minutes and then cooled down to room temperature. The black precipitate was separated from solution by filtering and washed to neutral with water and ultra pure ethanol and dried on oven in crucible with aluminum cover at 80°c for 5h. The ionic strength and temperature was effectively controlled and it was obtained the desired size and shape of NPs. Ionic strength controlled by keeping stoichiometric ratio of precursors during solution preparation and temperature was controlled by setting the temperature of hot plate. The pH of supernatant after decantation was measured by universal indicator. To synthesis of Fe_3O_4 was difficult without N_2 atmospheres but we try to synthesized it by covering the flask strongly by aluminum foil.

The **Humic acid coated Fe_3O_4 nanoparticles** was prepared following the same procedure except HA was added to modify the surface properties of bare magnetite.HA-Fe_3O_4NPswas synthesized by the co-precipitation method. Firstly the mass iron salts, $FeCl_3.6H_2O$ (6 g) and $FeSO_4.7H_2O$ (4 g) were measured using electronic balance in the stoichiometric ratio of (3:2) and dissolved in 100 mL water in conical flask and heated to 90^0C for three minute. Secondly, 15 mL of 25% NH_4OH was added gradually followed by stirring using magnetic stirrer until a black powder was formed in the solution. Then, 0.5 g of HA was dissolved quickly in 50mL of water and it was added rapidly and sequentially to the above solution. Because after formation magnetite NPs immediately aggregated and oxidized to the other form of iron oxides. Therefore insistu coating needed to control these properties.The mixtures was aged at 90^0C for 30 minutes and then cooled down to room temperature. The black precipitate was separated from solution by filtering and washed with water and ultra-pure ethanol and dried in oven by crucible with aluminum cover at 80 ºC for 5 h.The ionic strength and temperature was effectively controlled to get the desired size and shape of NPs.The effect of HA concentration on surface of magnetite NPs also was studied by varying the amount of HA added so that Fe_3O_4precursor to HA ratio in the final solution was(, 10:1) and 20:1) and labeled as HAC-1 and HAC-2, respectively [95, 96]. The pH of supernatant after decantation was measured by universal indicator

The reaction mechanism was as follows:

$$2FeCl_3.6H_2O + FeSO_4.7H_2O + 8\ NH_4OH \longrightarrow Fe_3O_4 + 6\ NH_4Cl + (NH_4)_2SO_4 + 23\ H_2O \quad (14)$$

$$Fe_3O_4 + HA \longrightarrow Fe_3O_4\text{-}HA \quad (15)$$

3.4. Characterization of humic acid coated magnetite nanoparticles (HA-Fe_3O_4)

Unlike conventional materials for which chemical composition and concentration are sufficient metrics, nanoparticles have different analytical requirements that must be measured for a complete description. This includes:

Physical characterization (size, size distribution, optical properties, crystal structure, morphology, and surface area of a specific Nanomaterials was characterized by SEM, XRD, UV-Vis spectroscopy and sear methods.

Chemical characterization (atomic composition, surface functional group, purity and reactivity) was characterized by EDX and FTIR Spectroscopy.

Behavioral characterization (particle stability (colloidal and dissolution) was tested by gravitational sedimentation method (Y ongchao Li, Z. X., (2013)..

3.4.1. Characterization Fe_3O_4/HA NPs by X-ray diffraction (XRD)

X-ray diffraction (XRD) analysis of the synthesized materials was done at ASTU research laboratory of Material science and engineering department. X-ray diffraction (XRD) patterns were measured by a (Shimadzu, XRD-7000S South Korea) Focus Diffractometre with Cu-Kα radiation (λ=0.15406 nm) operated at 40 kV and 30mA, with a scanning range from10^o to 80^o. This XRD line width can be used to estimate the size of the particle via the Debye– Scherer formula as described in the literature part

Sample preparation:- Approximately 2 g of as prepared as well as synthesized nanoparticles powders were finely grounded and filled in the sample holder and mounted on the X-ray diffractometre

3.4.2. Characterization humic acid coated magnetite NPs by FTIR

FTIR analysis of synthesized nano adsorbent was done at Addis Ababa University, Chemistry Department. The FT-IR spectra Fe_3O_4 and HA- Fe_3O_4 was obtained at between 400 cm^{-1} – 4000 cm^{-1}

Sample preparation: - The synthesized powdered powdered NPs were mixed with potassium bromide (KBr) as diluter to form a very fine powder. The powder was then compressed into a thin transparent pellet which is used for taking FTIR spectrum**.**

3.4.3. Characterization of Fe_3O_4/HA NPs by SEM-EDX

The external morphology, size and crystalline structure, percentage composition and orientation of materials making up of the nano sample were determined by scanning electron microscope**.** The Scanning Electron Microscope (SEM) produces images by detecting secondary electrons which are emitted from the surface due to excitation by the primary electron beam .The energy dispersive X-ray spectroscopy used for estimation of chemical composition of synthesized nanoparticles.

Sample preparation: - Small amount of powder sample was dispersed in acetone and sonicated for few minutes. Further, a drop of the mixture was spread on the conducting carbon tape pasted over the SEM stub. Further, thin layer of gold was coated using sputter coater for better conduction. Microstructure of the synthesized metal oxide powders was recorded at different magnifications.

3.4.4 .Characterization of Fe_3O_4 /HA by UV-Vis DRS Spectrophotometer

The optical properties and band gap energy of humic acid coated magnetite nanoparticles were characterized by UV-Vis DRS spectrophotometers. The range of absorption was between 180 nm to 800 nm. Optical properties characterize the response of materials to incident electromagnetic radiation.

Sample preparation: The sample was dissolved in appropriate solvent and fills in to sample holder caveat and used for analysis.DRS can also measure absorbance of solid powdered sample also used

3.4.5. Determination Stability of Fe_3O_4/HA NPs

The colloidal stability of humic acid coated magnetite NPs are a key factor in assessing transportability in aqueous solution was evaluated by gravitational sedimentation test. The setting test was conducted by adding 0.2 g HA-Fe_3O_4 (0.2 g) into a 20 ml comparison test tubes and observing its sedimentation property for 1day. For comparison the bare magnetite also done with the same procedure (Y ongchao Li, Z. X., 2013).

3.4.6. Determination of Surface Area of Fe_3O_4/HA NPs

The experiment was done according to sear method [98]. It was conducted by adding 0.5 g of NPs and 10 g NaCl in 250 ml conical flask and dissolved by 50 ml of distilled water. After that the PH of solution adjusted to 4 then the solutions titrated by 0.1 M NaOH until PH reach to 9. The volume of NaOH required to change PH 4 to 9 was record (Heidarizad M., Şengör S.S., 2016).

$S = 32V - 25$…….. (16)

Where S is specific surface area, V is the volume of NaOH solution in mL

3.5. Methylene Blue Removal by HA-Fe_3O_4 Nps in Aqueous Solution

3.5.1. Stock solution preparation

A stock solution with methylene blue concentration of 500 mg/L was prepared by dissolving 0.5 g of dye powder in 1000 mL volumetric flask filled with distilled water up to marks. Different dye concentration solutions (5, 10, 20, 30, and 40 mg/L) were prepared by serial dilution of concentrated stock solution. For the calibration curve the absorbance of the dye concentrations were measured by UV-Vis spectrometer at maximum wavelength of 665 nm.

3.5.2. Preparation of 0.1M NaOH and 0.1 M HCl

For the pH adjustment during the Bach adsorption experiment 0.1 M NaOH and 0.1 M of HCl were used. NaOH was prepared by dissolving 2 g of NaOH pellet in to 500 ml volumetric flask with in distilled water and HCl was prepared through serial dilution from stock solution by taking 4.2 ml of 12 M of HCl and diluted in to 500 ml volumetric flask by distilled water.

3.5.3. Bach Adsorption Experiment

The adsorption experiments were done according to (Qadri S., et al, 2009, Namasivayam C., Sumithra S., (2005).The preliminary test was done by taking 10 mg dosage, pH 9 and 25 ml of 10 mg/l initial dye concentration with the contact time 60 minute. This was due to MB exist in industrial effluent at small concentration and it is a cationic dye better removal efficiency attained at basic pH. The pH of solution was adjusted by 0.1M HCl and 0.1M NaOH solution until pH reach to 9. The solutions were shaken at room temperature (25℃) with a shaker speed of 100 rpm for about 60 minute. After a defined time intervals, the magnetic nanoparticles were removed from the solution by magnetic separator and filtration with what man filter paper. The absorbance of dyes left in the supernatant solutions after magnetic separation was determined by using UV-VIS spectrophotometer at a maximum wave length of 665nm.

Optimization experiments:-The experiment was optimized based on (Qadri S., et al, 2009). The adsorption experiment was conducted by varying pH (3, 7, 8, 9 and 11) because MB is a cationic basic dye and its removal by different adsorbent on the basic medium between PH 7-9.but PH 3 had been selected to study removal efficiency at acidic medium and to compare coated and bar magnetite removal efficiency of MB at this pH. The optimization also done by varying adsorbent dosage (10 mg, 15 mg,

20 mg, 25 mg and 30 mg) and contact time in minute (20 min, 40 min, 60 min, 80, min and 100 min) to gate maximum adsorption of the dye by coated nanoparticles. Parameters were increased or decreased in sequence manner to study their effect better. To test the effect of one parameter other parameters were hold constant.

Kinetics study:-The kinetics study was conducted at optimum pH of adsorption with the initial dye concentration of (20 mg/l) and 10mg/l at fixed adsorbent dosage (25 mg), room temperature ($25^{o}C$) with shaker speed of 100 rpm and adsorption was measured at any time t. Then all the calculations were done according to the equation described in the literature part.

4. Results and Discussions

4.1. Observed results during the synthesis of NPs

Up on mixing of $FeCl_3.6H_2O$ and $FeSO_4.7H_2O$ and dissolved in water a pale yellow color was observed. After heating of the mixture a pale red color was observed and 25% NH_4OH was added gradually followed by stirring using magnetic stirrer a black powder in the solution were formed. This black color precipitate indicates the formation of magnetite nano particles from Fe^{+2} and Fe^{+3} salts with ammonium hydroxide as precipitating agent. The PH of supernatant after decantation was measured by universal indicator which was 10-11 PH range. This indicates that magnetite was synthesized in the basic medium.

During the precipitation of Fe_3O_4 from $Fe^{2+}$and Fe^{3+}salts mixtures, two separate reactions could occur after addition of ammonium hydroxide to observe the precipitation of Fe_3O_4MNPs. It was well known that $Fe(OH)_2$ and $Fe(OH)_3$ formed at $pH > 8$ by the hydroxylation of the ferrous and ferric ions under anaerobic conditions (Namasivayam C., Sumithra S., 2005). Consequently, the formation of Fe_3O_4 MNPs occurred with black precipitation. The possible reaction for the formation of Fe_3O_4MNPs as follows:

- $Fe^{3+} + 3OH^- \longrightarrow Fe(OH)_3$ ……. …(17)
- $Fe(OH)_3 \longrightarrow FeOOH + H_2O$ …… (18)
- $Fe^{2+} + 2OH^- \longrightarrow Fe(OH)_2$…… (19)
- $2FeOOH + Fe(OH)_2 \longrightarrow Fe_3O_4\downarrow + 2H_2O$…… (20)

To modify the surface properties and to control oxidation and aggregation of magnetite NPs was prepared following the same procedure except HA was added to modify the surface properties of bare magnetite. The effect of HA concentration on surface of magnetite NPs also was studied by varying the concentration of HA in the ratio of precursors to HA (20:1, 10:1) which labeled as HAC-1and HAc-2. As compare to bare magnetite nano particles the coated nano particles can easily crashed by mortal this is due to humic acid can strongly prevent its aggregation and powdered Nps produced directly in the coated synthesis.

4. 2. Characterization of Synthesized NPs

4.2.1. X –Ray diffractometre (XRD) analysis of NPs

The XRD patterns of HAC-1, HAC-2 and Fe_3O_4NPs were shown in Fig 6. The pattern shows well defined peaks for all synthesized NPs, indicated that it is crystalline. The characteristic diffraction peaks of the synthesized magnetite were seen in 2θ = 30.253°, 35.6055°, 43.8914°, 53.7066° 57.2253°, and 62.8094° which are the reflection of (220), (311), (400), (422), (511) and (440) respectively (Fig. 6a,b,c). Diffraction peaks at d_{311} (2θ = 35.6055°) which were high and sharp observed on synthesized magnetite NPs which confirms the samples were purely magnetite. The XRD peaks are in accordance with the peaks characteristic of inverse cubic spinel structure in accordance to joint committee on powdered diffraction standards (JCPDS no. 00- 019-0629). The synthesized magnetite NPs had similar XRD spectra which were previously synthesized by different researchers in different literatures (M R Joya1,et al, 2013, Etolka tombacz, 2003).

The observed intense reflection at (311) plane in contrast to the other planes in Fig. 6 may specify the growth direction of the nano crystals. Moreover, the synthesized NPs were pure magnetite as the characterization peak of other iron oxides were not observed in the XRD spectra. For instance, the characteristic peak (major peak) of hematite (α-Fe_2O_3) is present: 33.45° (104), 36.02° (110) and 57.33° (122) (Petcharoen, K., and Sirivat, A., 2012). Whereas, those peaks were not observed in the XRD spectra of the synthesized NPs.The characteristic peaks for coated magnetite NPs were more or less similar to the bar magnetite but the peak intensity was decreased due to surface coverage by HA. This indicated that the crystal structure of $Fe_3O_4$was not changed after modification with HA.

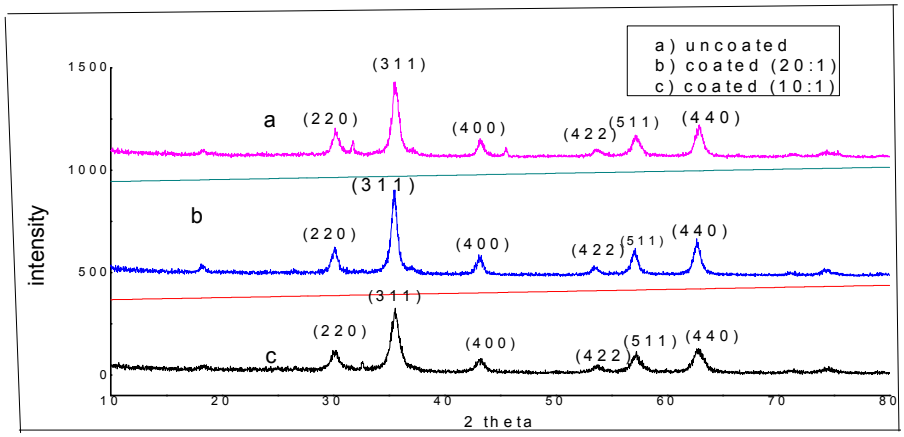

Figure 6 XRD spectra of magnetite NPs and humic acid coated magnetite NPs (a) Fe_3O_4, (b).HAC-1 and c) HAC-2

The size of the magnetite crystals and humic acid coated magnetite nanoparticles estimated using the Debye-Scherer equation based on the XRD data were given in Table 2. Crystallite size is a measure of the size of a coherently diffracting domain. Due to the presence of polycrystalline aggregates, crystallite size is not generally the same as the particle size. Crystallite size analysis on a sample containing extended defects can be used to estimate the ordered domain size (the size of the region between defects) in the same manner that XRD is used to determine crystallite size.

As shown in table 2, increasing humic acid concentration on the surface of bare magnetite resulted in NPs with smaller size crystal of 9.17nm.This is because of it speeds up crystal growth which leads to smaller size of NPs (Soerja Koesnarpadi, et al, 2017). But, use of small amount of HA led to the formation of larger particles size of 12.65 nm, due to the combination of the coating agent layers on the surface of Fe_3O_4 (Teja A.S, and Koh P.Y., 2009).

The lattice constant, or lattice parameter, refers to the physical dimension of unit cells in a crystal lattice. Lattices in three dimensions generally have three lattice constants, referred to as a, b, and c. However, in the special case of cubic crystal structures, all of the constants are equal and we only refer to a. A group of lattice constants could be referred to as lattice parameters. However, the full set of lattice parameters consist of the three lattice constants and the three angles between them. The lattice parameters of synthesized magnetite NPs and Humic acid coated magnetite NPs were calculated by the following formula (Cao, S.-W., et al, 2009).

$d_{(hkl)} = \frac{a}{\sqrt{(h^2+k^2+l^2)}}$ ..... (21) Where, $d_{(hkl)}$ is D-spacing of major peaks at miller index of (hkl), α is lattice parameters. The reflection peaks in the pattern can be indexed to face centered cubic phase and majored peak miller index (d_{311}) and D-spacing (2.51945 A^o and 2.52779 for uncoated and coated magnetite NPs respectively)

The calculated lattice parameters of synthesized magnetite NPs and Humic acid coated magnetite NPs were a=8·356Å and 8.384Å, respectively. This result was in agreement with the bulk lattice parameter of Magnetite (a=8·39 Å) (Jain T.K, et al, 2005). Because the bulk lattice parameters of other iron oxides like Maghemite (8.34 A^o) and Hematite (5.46 A^o) are less than the value obtained in magnetite. Therefore the synthesized NPs were purely magnetite NPs.

Table 2. The calculated crystal size of bare magnetite and HA coated magnetite NPs

sample type	major peaks(2 theta value(deg.)	theta value	Beta (β) value (degree)	β in radian	average crys size
Fe_3O_4	35.6055	17.803	0.7285	0.012719841	11.2nm
	62.8084	31.404	0.81	0.014142857	
	30.253	15.1265	0.74	0.012920644	
HAC-1	35.5326	17.76663	0.8787	0.015342381	9.17nm
	62.7833	31.39165	1.0467	0.018276	
	30.13	15.065	0.86	0.015015873	
HAC-2	35.4841	17.74205	0.6267	0.010942381	12.65nm
	62.6555	31.3275	0.704	0.012292206	
	30.1385	15.0691	0.69	0.012047619	

4.2.2. Forier Transfer Infrared spectroscopy (FTIR) analysis

The FTIR spectra of as synthesized humic acid coated magnetite and bar magnetite NPs samples were shown in Figure 6. The broad band around ~3423cm^{-1} (Figure 7) corresponds to stretching indicating the existence of small amount of water adsorbed to the NPs (Chakrabarti, S., et al, 2009). The peak around ~2909 $cm^{-1}$and ~2854 $cm^{-1}$are assigned to residual organic component asymmetric and symmetric C-H stretch-mode frequencies, respectively. The peak around ~2337 cm^{-1} and 2400 cm^{-1} arises from the absorption of atmospheric CO_2 on the metallic cations (Farmer V. C., et al, 1982). The band at ~1617 cm-1 could be associated with the bending vibrations of water molecules. The absorption band around ~ 1400 $cm^{-1}$and 1387 cm^{-1}corresponds to asymmetric stretching of C=O bonds of the CO_2which might remain adsorbed on the surface of magnetite during drying. The peak around ~1129 $cm^{-1}$and ~1100 cm^{-1}could is due to bending vibration of C=O. The peak appearing at around 594 cm^{-1} is assigned to the metal- oxygen (Fe–O) stretching modes (.Weber T.W., R.K., 1974). The FTIR spectra of this synthesized nanoparticles accordance with the previous synthesized magnetite NPs by different researchers (Maity D., and Agrawal C., 2007, Carlos, L., et al, 2012, Maity D. and Agrawal C., 2007).

As shown in the Figure 7 the FTIR spectra of uncoated magnetite and humic acid coated magnetite had nearly similar but the coated magnetite had very broad band spectra around 3454$cm^{-1}$and a very long

spectra around 1632cm^{-1} as compared to uncoated NPs. This was due to the carboxylate acid, alcohol function group and the aromatic nature of humic acid respectively. The spectroscopic analysis of HA from Fe_3O_4/HA with the mass ratios of 20:1and 10:1 are shown Fig.7. FTIR spectra of HA coated Fe_3O_4 indicated the presence of O-H stretching vibration at 3454 cm^{-1}, the wave number of 1632 and 1395 cm^{-1}attributed to the C=O stretching vibration on COOH and COO asymmetric stretching vibrations and aromatic C=C stretching vibration respectively. Both of Fe_3O_4 and Fe_3O_4/HA centered at 578 cm^{-1}were attributed to the stretching vibration of Fe-O bond (Weber T.W., R.K., 1974).The successful coating of HA on Fe_3O_4 showed the C=O vibration at 1395 cm^{-1}, indicating that the carboxylate anion interacted with the Fe_3O_4 surface as the C=O vibration in free carboxylate acids is around 1700 cm^{-1} and this suggests that carboxylate groups indeed play an important role in the bonding between HA and Fe_3O_4 (Soerja Koesnarpadi, et al 2017). It is believed the bonding between HA and Fe_3O_4 surface is mainly done through ligand exchange. In general as shown in the spectra humic coated magnetite have high peak intensity due to the multi functional group of coating material humic acid.

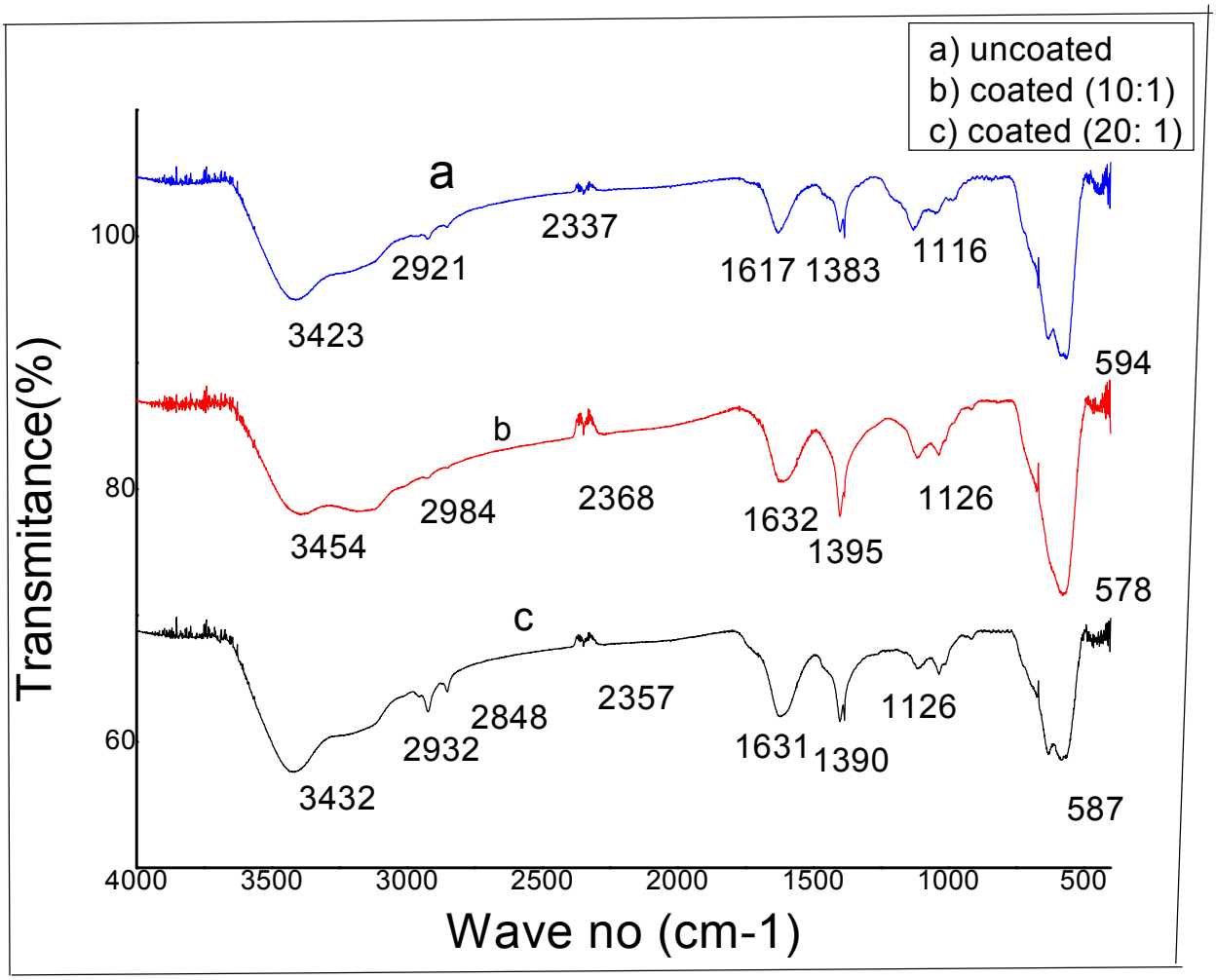

Figure 7.FTIR spectra of (a) Fe_3O_4 (b) HAC-1, and (c) HAC-2

4.2.3. UV-Vis DRS analysis of synthesized NPs

The band gap energy of synthesized nanoparticles was estimated by ultra violet visible diffuse reflectance spectroscopy (UV –Vis DRS). The band gap is the minimum energy needed for an electron to be excited from the top of the valence band to the bottom the conduction band once that minimum energy is reached (the band gap energy), then the sample can start absorbing light and electrons are excited from the valence band to the conduction band.

UV-Vis DRS reflectance spectra of both synthesized Fe_3O_4 NPs and humic acid HA/Fe_3O_4 were shown in Figure 8. As shown from the figure bare magnetite had the greatest band gap energy (3.24 ev) than humic acid coated magnetite nanoparticles (3.2 ev for HAC-1 and 3.18ev HAC-2)).This is due to the magnetite surface is covered by coating material humic acid which might be decrease the incident light absorption by the sample. As shown from the graph the concentration of humic acid increases, the absorption intensity of synthesized Fe_3O_4 NPs also increases. This is due to humic acid had high

chromophoric group that absorbed the UV light and the smaller crystal size of nanoparticles. As the crystal size is very small the capacity to absorb incident light increase which leads to increasing the band gap energy. As shown from the reflectance graph increasing % of reflectance means decreasing absorbance and lower reflectance means higher absorbance. The maximum wavelength of Fe_3O_4, HAC-1 and HAC-2 were 320 nm, 371 nm and 374 nm respectively. The determination of optical band gap was obtained by Tauc's equation (Wang, M.D., et al, 2008).

$(\alpha h\nu)^{1/n} = A\,(h\nu - Eg)$ ……(22)

Where, α is a absorption coefficient constant, hν , is photon energy, Eg is the allowed energy gap, n = ½ for allowed direct transition and n = 2 for allowed indirect transition..The Tauc's region is extrapolated to $(\alpha h\upsilon)^2 = 0$ to obtain the band gap. The tauc graph plots the $(\alpha h\nu)^2$ vs. hν for both bare magnetite nanoparticles and humic acid coated magnetite NPs.

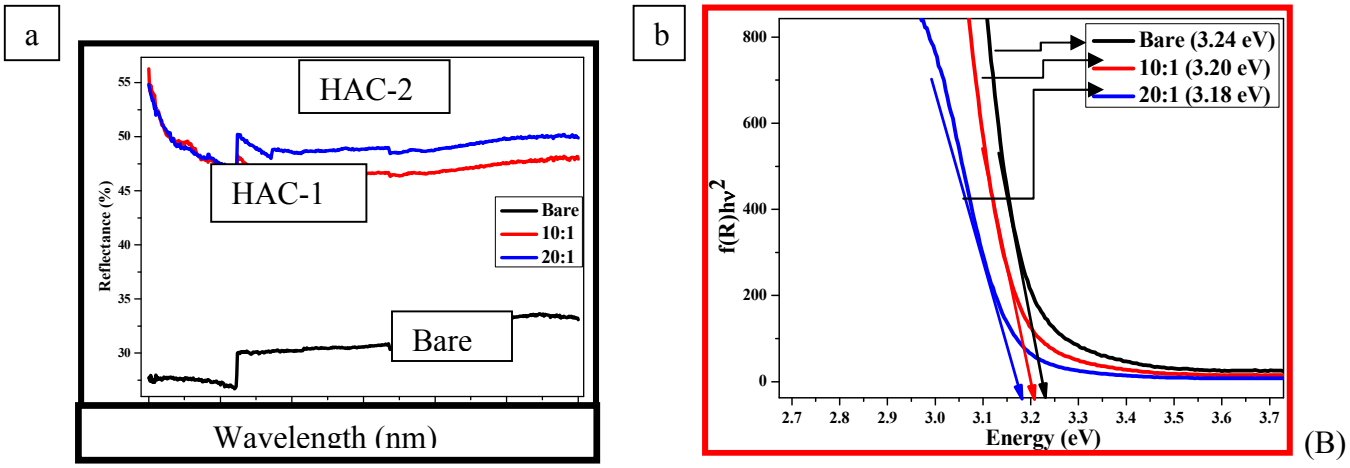

Figure 8 (A). % of Reflectance of both HA coated magnetite and bare magnetite NPs (b) Tauc plot from UV-Vis DRS band gap energy of humic acid coated magnetite and bare magnetite (Fe_3O_4)

As described above the band gap energy of a particle depend on crystal size due to this nanoparticles had high band gap energy as compare to their bulk matter because nanoparticles had high surface area to volume ratio that helps to absorbs the incident light [114]. There for the band gap energy of bulk magnetite is in the range of 1.8 eV to 2.8 eV since for this study the synthesized magnetite nanoparticles had high band gap energy as shown in the tauc plot graph.

4.2.3. Scanning Electron Microscope (SEM) NPs analysis

Scanning electron microscopy (SEM) is one of the most versatile instruments available for the examination of the morphology of solid materials including magnetite NPs and humic acid coated magnetite NPs. The surface morphology of the synthesized samples was viewed through the high resolution scanning electron microscope.

SEM images of bare magnetite and humic acid coated magnetite Nps were presented in Figure 9. As shown from the figure the SEM images of both bare magnetite and humic acid coated magnetite had pure a spherical morphology. As observed from the SEM image, the bar nanoparticles and HAC-2 had aggregates than that of HAC-1. This shows that high composition of HA could strongly prevent aggregations of magnetite NPs.The humic acid coated magnetite NPs had a homogeneous surface less aggregated than bar magnetite. This may be due to the high surface energy of the bar magnetite nanoparticles; on the other hand, high concentrations of the nanoparticles were deposited on the SEM grids which affected the image. The surface morphology of the synthesized NPs had accordance with the morphology of magnetite NPs which investigated by different researchers (Tombacz, E, et al, 2006, Carlos, L., et al, 2012).

The particle distribution of the bare magnetite is in the size range of 29-50 nm (Figure 9a) where as the particle distribution of humic acid coated magnetite was in range of 32-47 nm. This shows that the particle distribution of humic acid coated magnetite were homogeneous. More over the humic acid coated nanoparticles had higher porosity as compare to the bare magnetite NPs. This porosity were used as active site for contaminates to bind during application.

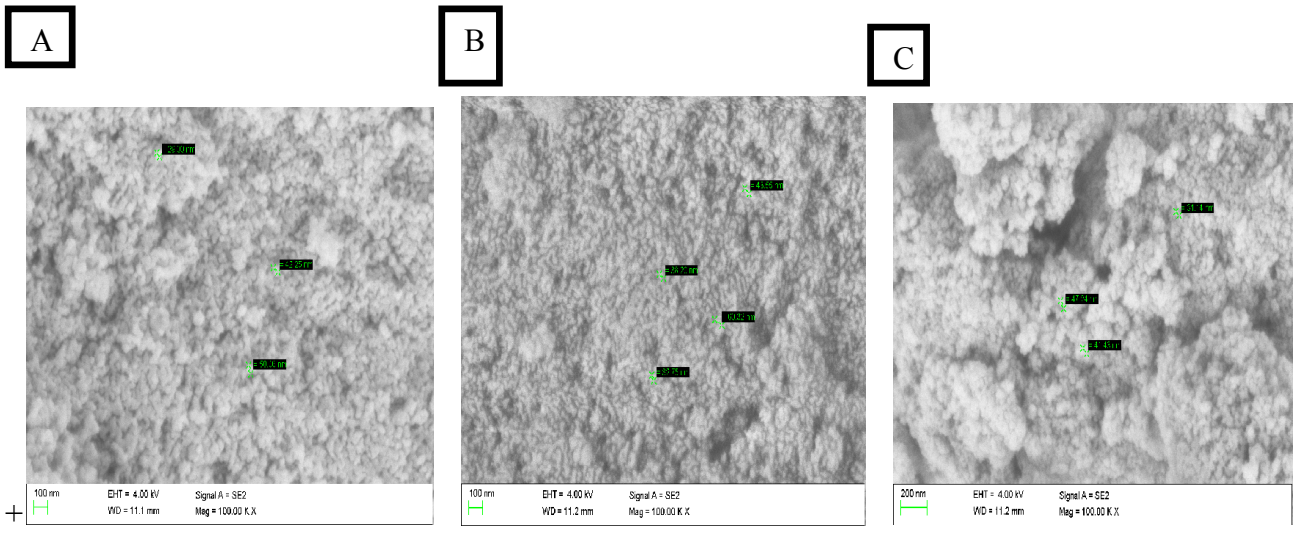

Figure 9 Scanning Electron Micrograph (SEM) Image of a).Fe_3O_4, b). HAc-1, c). HAc-2

4.2.4. Energy Dispersive X-Ray Spectroscopy (EDX) Analysis

The energy dispersive X-ray analysis of bare magnetite and HA/Fe_3O_4 ((HAc-1) and (HAc-2)) particles were shown in Figures 10. It is evident from the X-ray patterns of all the samples in which Fe and O are found in the respective spectra for all synthesized NPs. The energy dispersive X - ray spectroscopy (EDX, Fig. 9 a, b and c) analysis showed the strong peaks at 0.8, 6.3, and 6.8 keV confirmed that the presence of Fe in the synthesized NPs, (silica (Si) at 1.8 keV, Aluminum (Al) at 1.6 ev and oxygen (O) at 0.8keV.

The smaller amount of Si and Al peak were observed due to glass substrate used for film preparation or Detector of EDX. Because there is no characteristic peak of silicon and aluminum observed from the XRD spectra of synthesized nanoparticles. If silicon present in the sample around 2θ value of 26 ^{o} major peak of silicon should be observed. Furthermore, in the FTIR analysis also there is no silicon oxygen stretching peak observed because Si-O stretching should be observed around 900cm^{-1} to 1000 cm^{-1}.This clearly shows such type of interface comes during sample preparation. It might be the sample preparation glass made from aluminum silicate. Such types of interference have been viewed by different researchers and it was reported in different literatures (Wang Y., et al, 2009, Anbalagan Krishnasamy, et al, 2015). The impurity chlorine comes from the precursors which remain during drying of NPs in oven.

As shown from the EDX spectrum of humic acid coated magnetite NPs had high carbon content as we have seen bare magnetite NPs had not any carbon in its EDX spectrum. The C peak indicates the presence HA on the surface of magnetite nanoparticles. This indicates that humic acid was effectively coated on the surface of magnetite by ligand charge reaction. The carbon peak in HAC-1 was greater than HAC-2 due to the HA composition in HAC-1much greater than HAC-2.

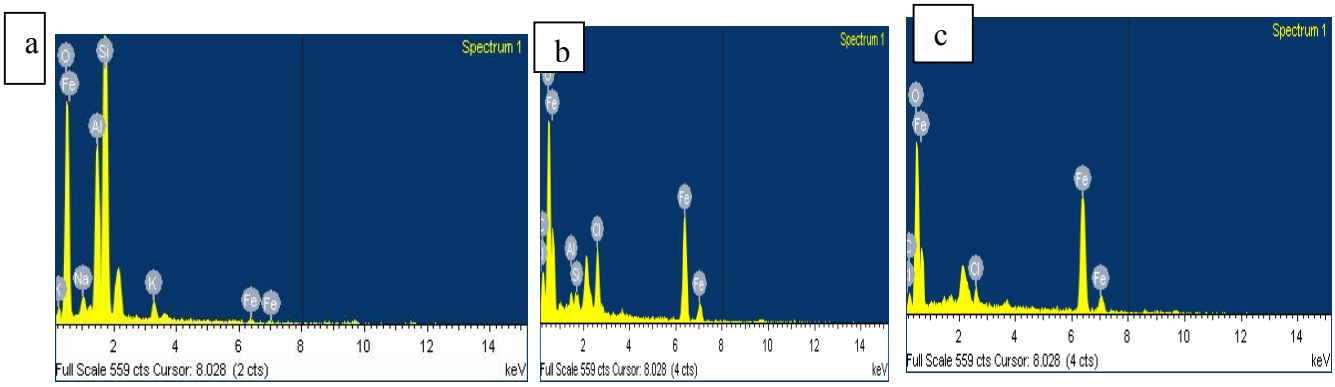

Figure 10. Energy dispersive x-ray spectra of a). Fe3O4. B). HAC-1 and c). HAC-2

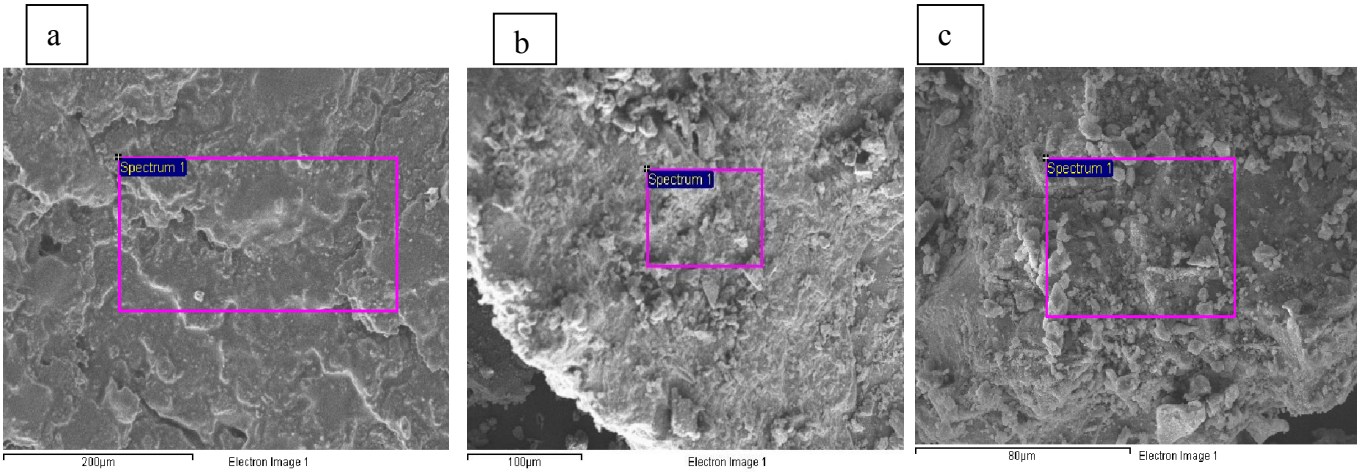

Figure 11.SEM images of selected area for EDX spectra of a). Fe_3O_4 b). HAC-1 and c).HAC-2

4.2.5. Determination of Stability of HA/Fe_3O_4

The colloidal stability of synthesized NPs were shown in figure 12. As shown in the figure 11(1^{st} test tube HAC-2, 2^{nd} bare magnetite and 3^{rd} HAC-1) the humic acid coated magnetite Nps were stable because it was suspension or it remain dispersion in the solution for about 1 dyes but for non coated NPs immediately form sediment in the solution as result some of the active site of NPs is hidden and decrease its application. In Humic acid coated magnetite NPs all the active site were free, to contact with the contaminant easily.

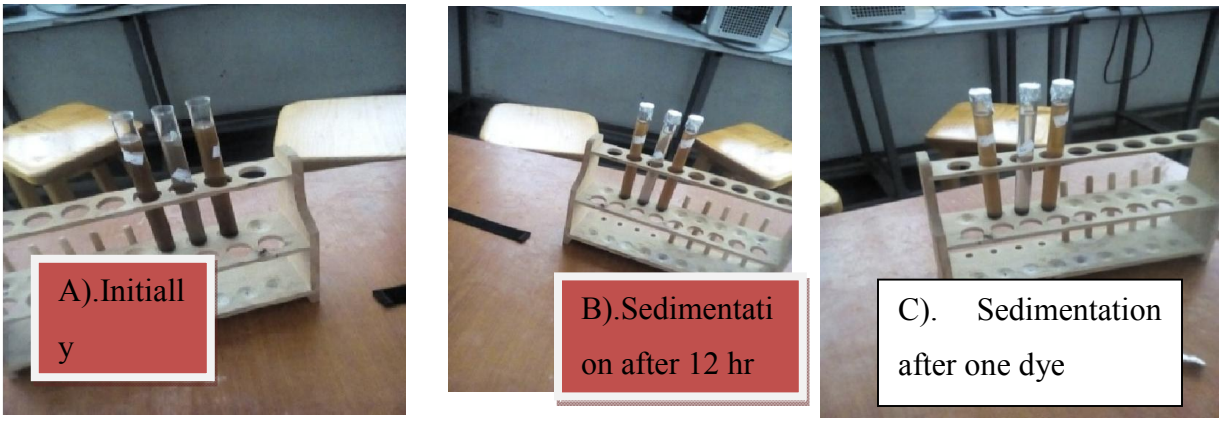

Figure 12. Stability test of HA coated and uncoated magnetite NPs initially (A), after 12 hr (B), after 1day (C)

4.1.4. Specific surface area

The specific surface area is increased as the particle size becomes small. However the specific surface area is also increased if the particle has pores. Even with the same material that has the same weight and volume, the surface activity and adsorption volume are changed according to the specific surface area.

So it is important to measure the specific surface area to evaluate the activity and adsorption capacity of materials. As shown from the table 3 the surface area of HAC-1 was greater than HAC-2 .This was due to the smaller crystal size of HAC-1.

Table 3.Sear method surface area calculation

No.	Type of NPs	Volume of NaOH consumed (mL)	Specific surface area (m^2/g)
1	Bar magnetite	8.5	247
2	HAC-1	10	295
3	HAC-2	8	231

4.2. Adsorption Experiment

Calibration curve for standard solution were done by various concentrations (5 mg/l, 10 mg/l, 20 mg/l, 30 mg/l). The experiments were repeated two times and the average data were used to plot the resultant graphs. A calibration curve of absorbance against MB concentrations was then plotted. The experimental data reported in Figure 13 were fitted by a straight line with a high regression coefficient value (R^2= 0.95).

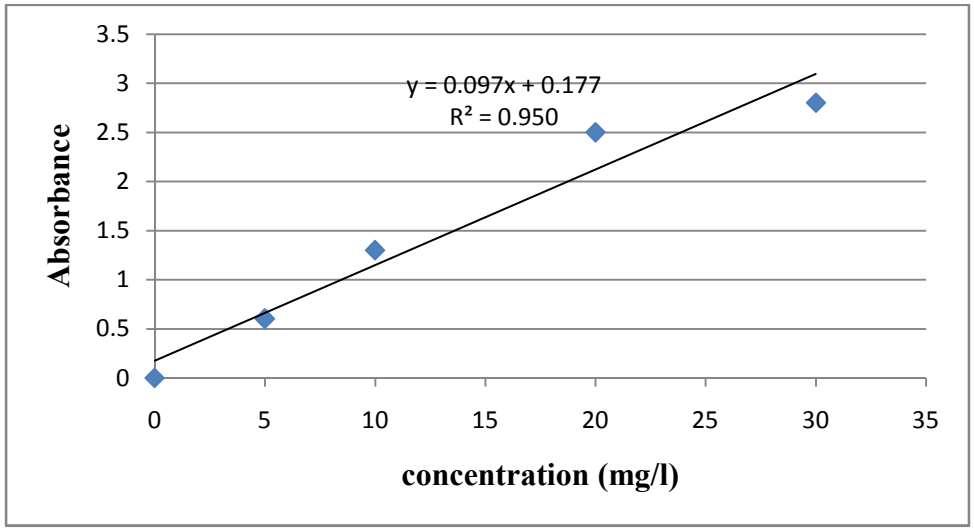

Figure 13 Calibration graph for standards

4.2.1. Optimization response

4.2.1.1. PH effect

Figure 14 shows the effect of initial pH on MB adsorption onto Fe_3O_4, HAC-1and HAC-2. The adsorption of MB onto magnetite NPs and Humic acid coated magnetite nano particles were intimately dependent on pH of solution. The adsorption capacity of MB on Fe_3O_4 and HAC-2 increases with increasing solution pH from 3.0 to 9.0, and changes slightly when solution pH is above 9.0 but for HAC-1 increase from PH 3 to 7 and changes slightly when solution pH is above 7.0 . This was due to the competence of OH^- ion with adsorbent site. As shown in the figure 13, humic acid coated magnetite NPs had high removal efficiency at acidic medium PH 3 as compare to bare magnetite NPs which is 66.7% and 85.8 % respectively this is due the external negatively charged and aromatic nature of coating material known as humic acid.

In addition, lower adsorption of methylene blue at acidic pH might be due to the presence of excess H^+ ions competing with MB cations for the available adsorption sites which reduce the adsorbed amount. Increasing the pH values from 3-7 and 3 to 9 was lead to deprotonation of the acid sites on magnetite surface and the surface becoming negatively charged with high attractive properties. This leads to increase in the surface diffusion of the dye molecules due to high the electrostatic interactions between MB and coated magnetite (Weber T.W., R.K., 1974, Qadri S., Ganoe A., et al, 2009).The optimum PH attained at PH 9 and 7 for Fe_3O_4, HAC-2 and HAC-1 with a removal efficiency of 85.2, 94.4 and 96 respectively.

According to different literature the PZC of magnetite was 7.9 and when it coated with humic acid PZC decreased from the original which was around 6. When the solution pH is below pHPZC, the Fe_3O_4 acquire a positive surface charge. The competitive effects of H^+ ions and the electrostatic repulsion between the cationic dye.

A)

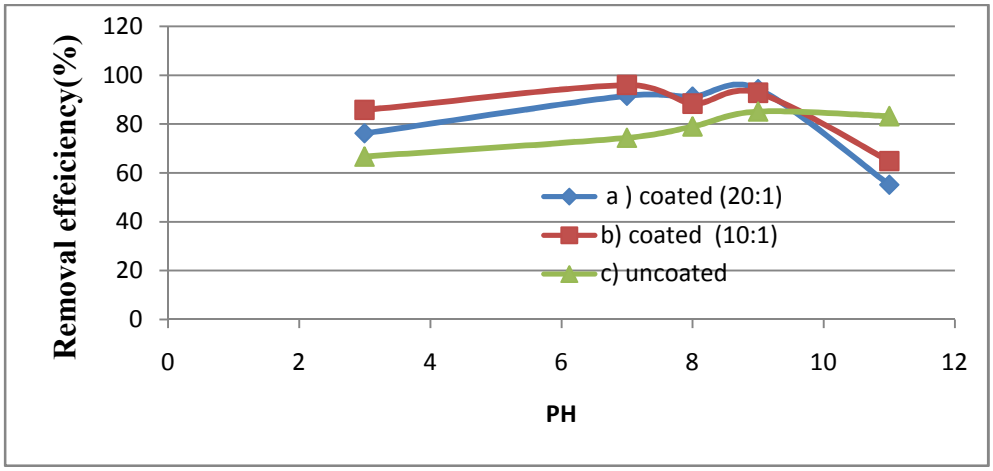

B)

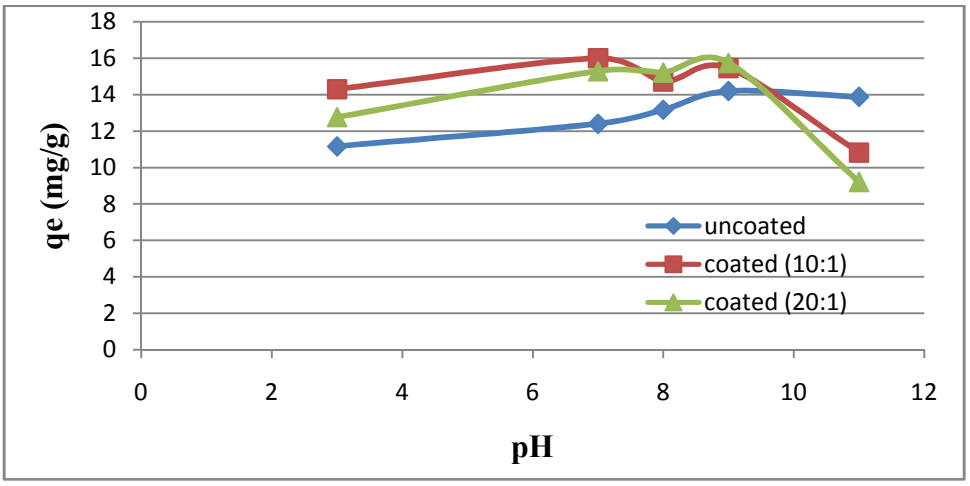

Figure 14.PH effect on (A) Removal efficiency (%), (B). adsorbent capacity (mg/g) at dosage =15 mg, contact time = 60 min. concentration =10mg/l V =25 ml, room temperature and with shaker speed of 100 rpm

4.2.1.2. Effect of Adsorbent dosage

As shown in the **figure 14** as increase in adsorbent dose from 10 mg to 25mg) the removal efficiency of MB also increase but above 25 mg the removal efficiency slightly decrease because increasing the adsorbent amount reduces the un saturation of the adsorption sites and correspondingly, the number of such sites per unit mass comes down resulting in comparatively less adsorption. Also this decreases the driving forces for adsorption (conc. of dye molecules/ conc. of adsorption sites) which decrease the dye diffusion from solution into the adsorbent platelets. In addition, overlapping of adsorption sites as a

result of over-crowding of adsorbent particles can decrease the removal efficiency of the adsorbent (Heidarizad M., Şengör S.S., 2016).The adsorption capacity of adsorbents were decrease with in increasing adsorbent dose because at higher dosage the ratio of adsorbed dye on adsorbent to the mass of adsorbent smaller. As shown from the graph the maximum removal efficiency attained at 25 mg of adsorbent.

A)

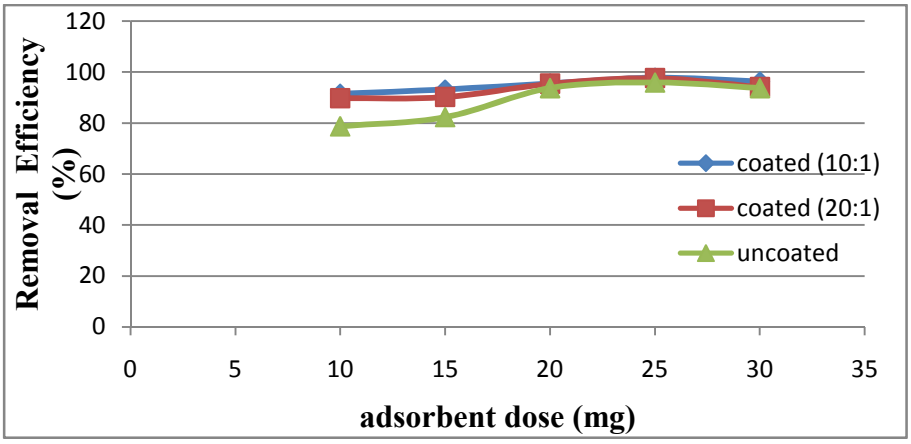

B)

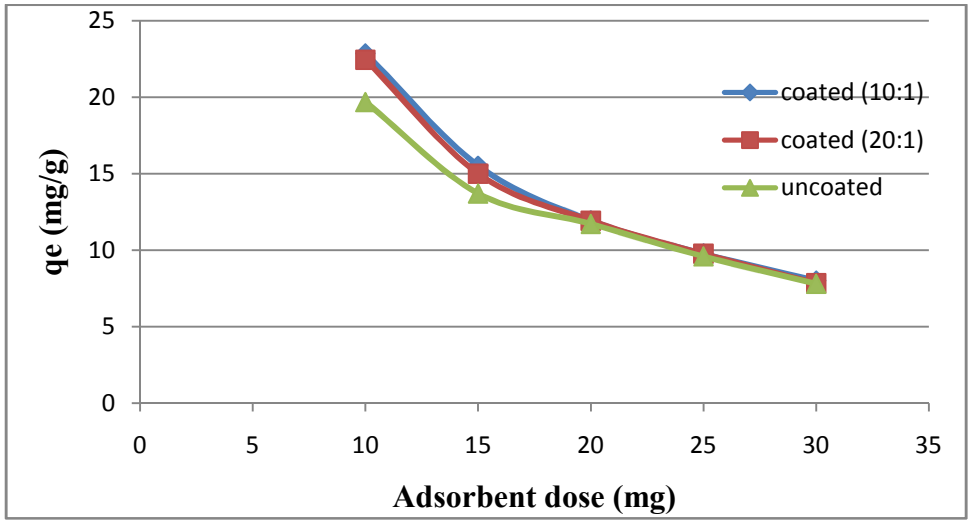

Figure 15. Effect of adsorbent dosage on (A) removal efficiency (%), (B) adsorbent capacity (mg/g) at fixed (concentration = 25 ml of 10 mg/l dye, time = 60 min., pH =9 for Fe_3O_4 and HAC-2 , PH 7 for HAC-1, Room temperature and shaker speed 100 rpm for all adsorbent.

4.2.1.3. Effect of initial concentrations

To optimize the initial concentration of dye on the adsorption process, experiments were conducted with. As shown in the figure 15 the adsorption capacity of MB increases with increasing initial concentration of dye but the percent removal of MB decreases with the increase in initial concentration suggesting that the adsorption of MB onto is highly dependent on initial Concentration.

The initial dye concentrations provide an important driving force to overcome the mass transfer resistance of the dye between the aqueous phases and the solid phases, so increasing initial concentrations would enhance the adsorption capacity of dye. On the other hand, the dye adsorption process generally involves the first transport of dye molecules from bulk solution through liquid film to the exterior surface of adsorbent and then from the exterior surface to the pores of the adsorbent, which reflects the adsorption of dye onto the adsorbent is relevant to the initial concentration. In general, the total number of available adsorption sites is fixed for a given adsorbent dose (Indira T.K, Lakshmi P.K., 2010, Wei Y., et al, 2012).

It is reasonable to particulate that the larger ratio of active adsorption sites of the adsorbent is available at lower initial concentration. Therefore, the percentage removal of dye is greater at lower initial concentration but smaller at higher initial concentration. Even though, at very small concentration removal efficiency is decreased because due to high available site immediately dye adsorbed at small equilibrium time but with in increasing time it desorbed (dissolution from the adsorbent) this leads to decrease removal efficiency. As shown from the graph the optimum initial concentration attained at a fixed dose was 10 mg/l with removal efficiency of 98.6 %, 95.5 % and 94.5% for HAC-1, HAC-2 and Fe_3O_4 respectively.

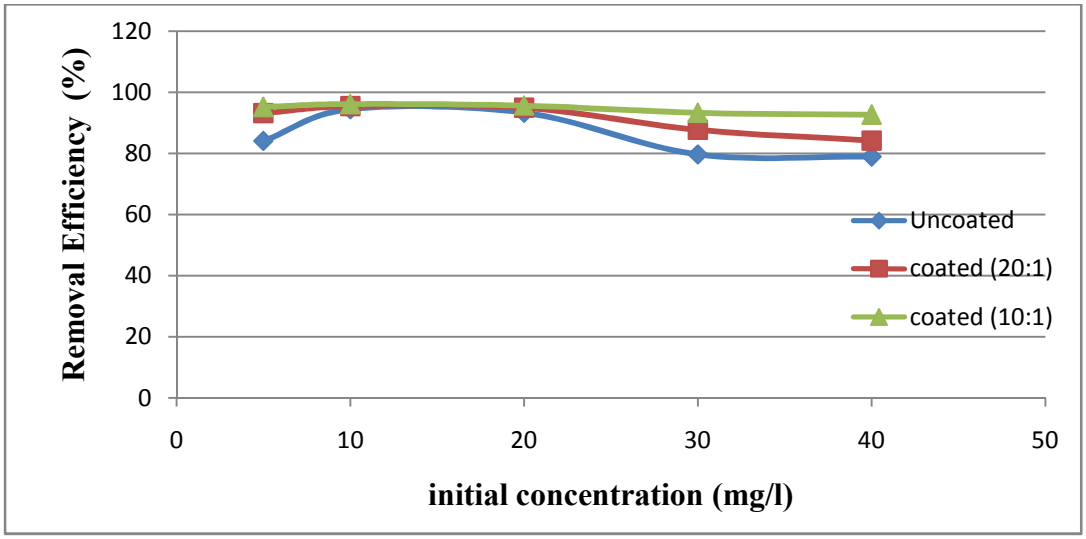

B)

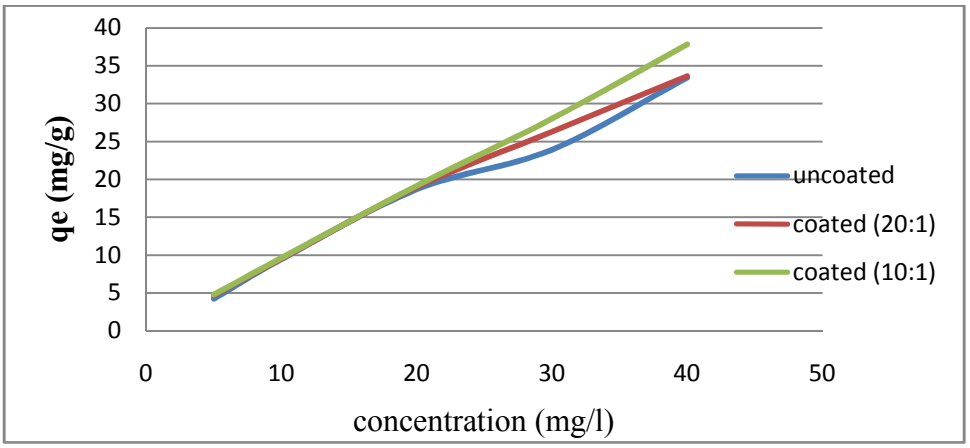

Figure 16. Effect of initial concentration on (A) removal rate (%) (B). Adsorbent capacity (mg/g) at 25 mL of (5 mg/l, 10 mg/l, 20 mg/l, 30 mg/l and 40 mg/l) concentrations with fixed (dosage =25 mg, pH = optimum for all adsorbent, contact time 60 min

4.2.1.4. Effect of Contact time

Figure16 shows the effect of contact time on the adsorption capacity and percent removal of MB onto the synthesized NPs at the same initial concentrations (10 mg/l). The adsorption capacity and percent removal of MB onto the Fe_3O_4 and HA/Fe_3O_4 drastically increase during the initial adsorption stage and then continue to increase at a relatively slow speed with contact time until a state of equilibrium is attained which was 60 min and 80 min for Fe_3O_3, HAC-2 and HAC-1 with a removal efficiency of 95.8%, 97.8%, and 99.6% respectively. This phenomenon is attributed to the fact that a large number of vacant surface sites are available for adsorption at the initial stage, and after a lapse of time, the

remaining vacant surface sites are difficult to be occupied due to repulsive force between the solute molecules on the solid and bulk phases (Wei Y., etal, 2012). As shown from the figure the adsorbent capacity increases with increasing contact time until reach to equilibrium time with the maximum adsorbent capacity of 9.96 mg/g.

A)

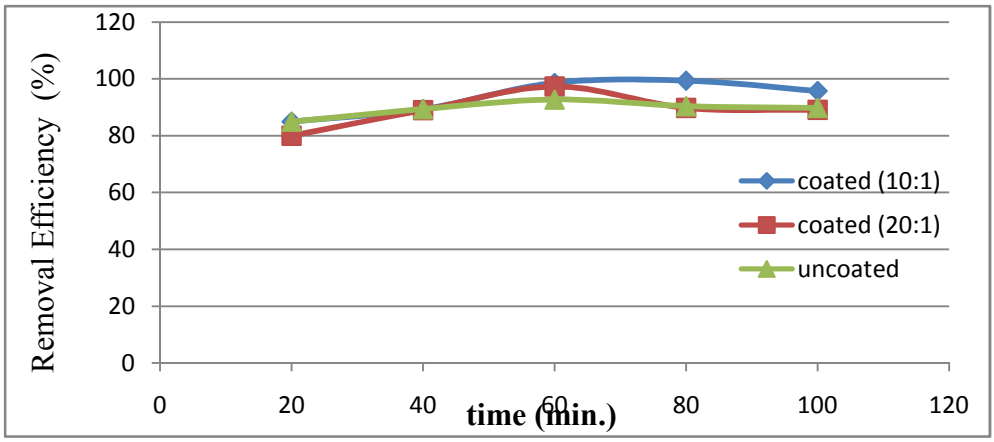

B)

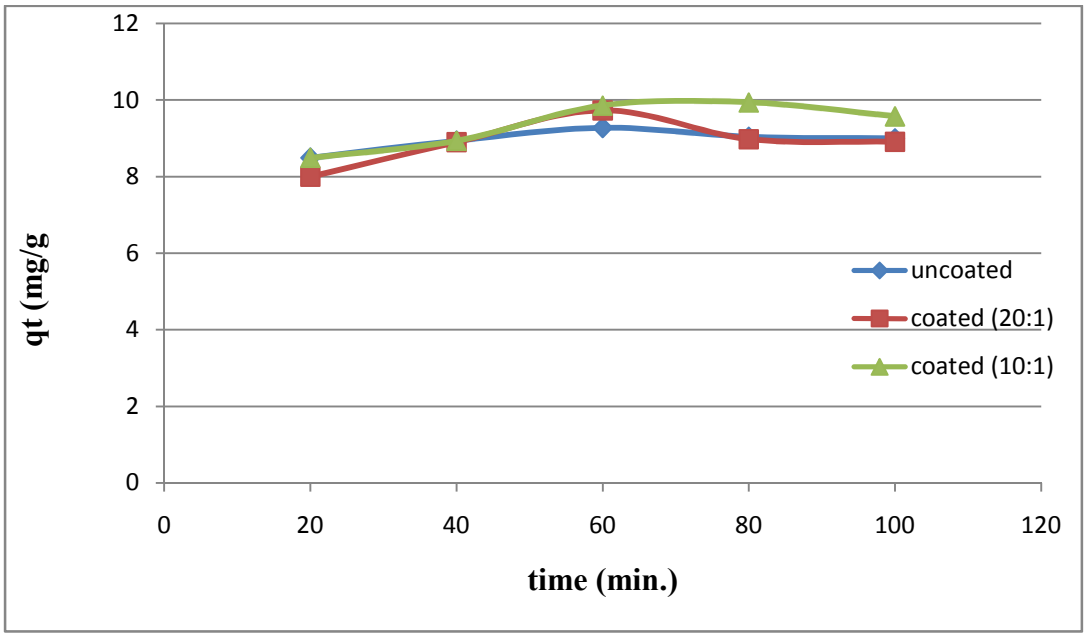

Figure 17. Effect of contact time for on (A) .Removal rate (%) (B), adsorbent capacity (mg/g) various contact time (20 min, 40 min, 60 min, 80 min and 100 min.) at fixed (dosage =25 mg, pH = optimum for both adsorbent, 25 ml of 10 mg/l of initial concentration, room temperature and shaker speed of 100 rpm

4.2.2. Kinetics study

Kinetic models have been exploited to test the experimental data and to find the mechanism of adsorption and its potential rate-controlling step that include mass transport and chemical reaction. In addition, information on the kinetics of dye uptake is required to select the optimum conditions for full scale batch or continuous dye removal Processes. Adsorption kinetics is expressed as the solute removal rate that controls the residence Time of the sorbate in the solid–solution interface. In order to further understand the characteristics of the adsorption process, the pseudo-first-order and pseudo-second-order kinetic models were applied to fit experimental data obtained from batch experiments. The pseudo-first-order and pseudo-second order kinetic models are expressed in nonlinear form as follows.

4.2.2.1. Pseudo-first-order kinetic model

To determine if the adsorption process fits with pseudo-first order model or not the experimental data were done at different concentration (25 ml of 10 mg/l and 20 mg/l) at fixed dosage (25mg), pH optimum for both and contact time (10 - 60 min) with 10 min interval and room temperature at shaker speed of 100 rpm. The rate constant and qe (cal) was calculated from the slope and intercepts of the graph log (qe-qt) vs. time graph. The kinetics graphs of all adsorbent were shown in figure 17. As shown from the figure the sorption kinetics of MB removal Fe_3O_4 and Fe_3O_4 /HA (Figure 17) were not predicted by pseudo first order kinetics model since calculated and experimental dye removal were not close to each other as it can be seen from the Table 6.

A)

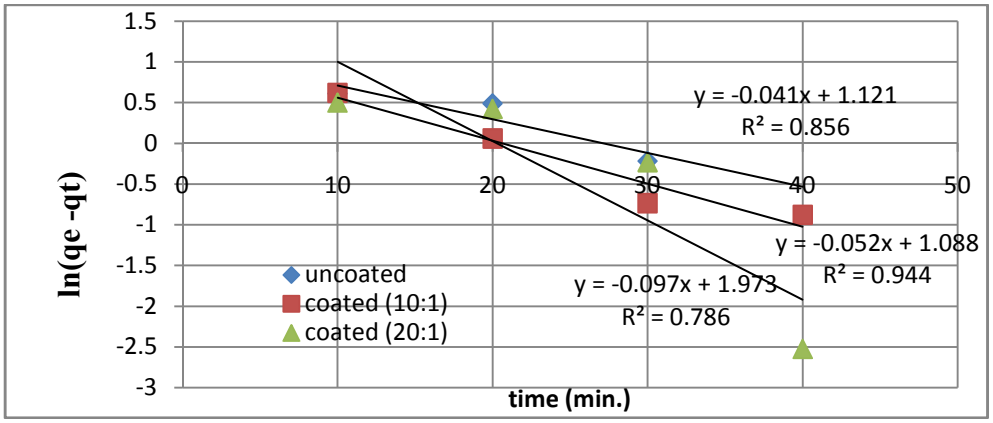

B)

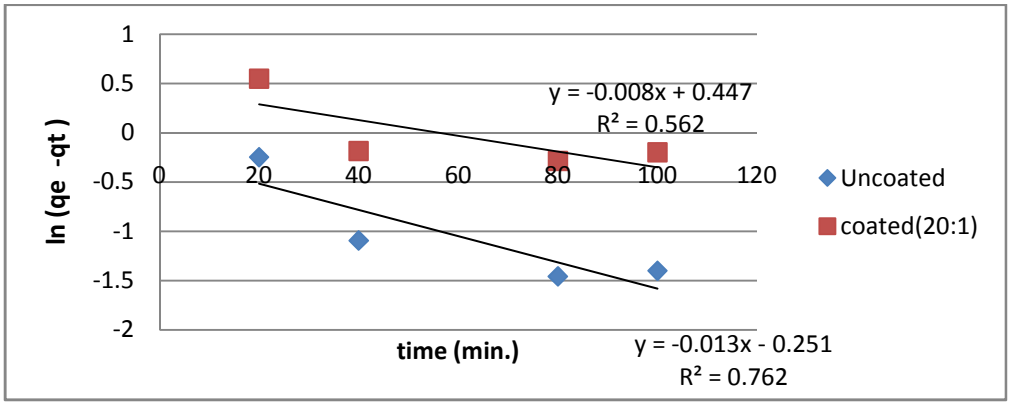

C)

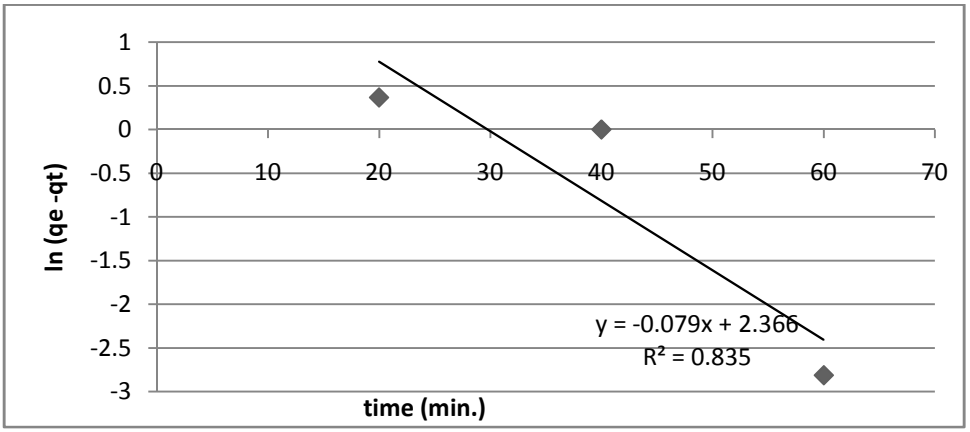

Figure 18. Pseudo 1st order kinetics (A).at 20mg/l for all (B).at 10mg/l for both HAC-2 and uncoated magnetite, (C), for HAC-1

4.2.2.2. Pseudo second-order kinetic model

In this model, the rate-limiting step is the surface adsorption that involves chemisorption, where the removal contaminant from a solution is due to physicochemical interactions between the two phases (Hu C.H, et al, 2009).

The plot of t/qt Vs t should give a linear relationship from which qe and K_2 can be determined from the slope and intercept of the plot respectively. Fig.18. Shows the pseudo second order kinetics at different concentration (10 mg/l and 20 mg/l). As shown in the graph the experimental data for sorption kinetics of MB removal by Fe_3O_4/HA were strongly fitted to pseudo second order kinetics model because the calculated and experimental dye removal were very close to each other as it can be seen from the Table 4.The qe (cal) and rate constant was calculated from the slope and intercepts of the graph t/qt vs. time graph. As shown from the table the reggration coefficient of pseudo second order kinetics greater than pseudo first order kinetics this indicates pseudo 2nd order more describe the batch adsorption mechanism of this study.

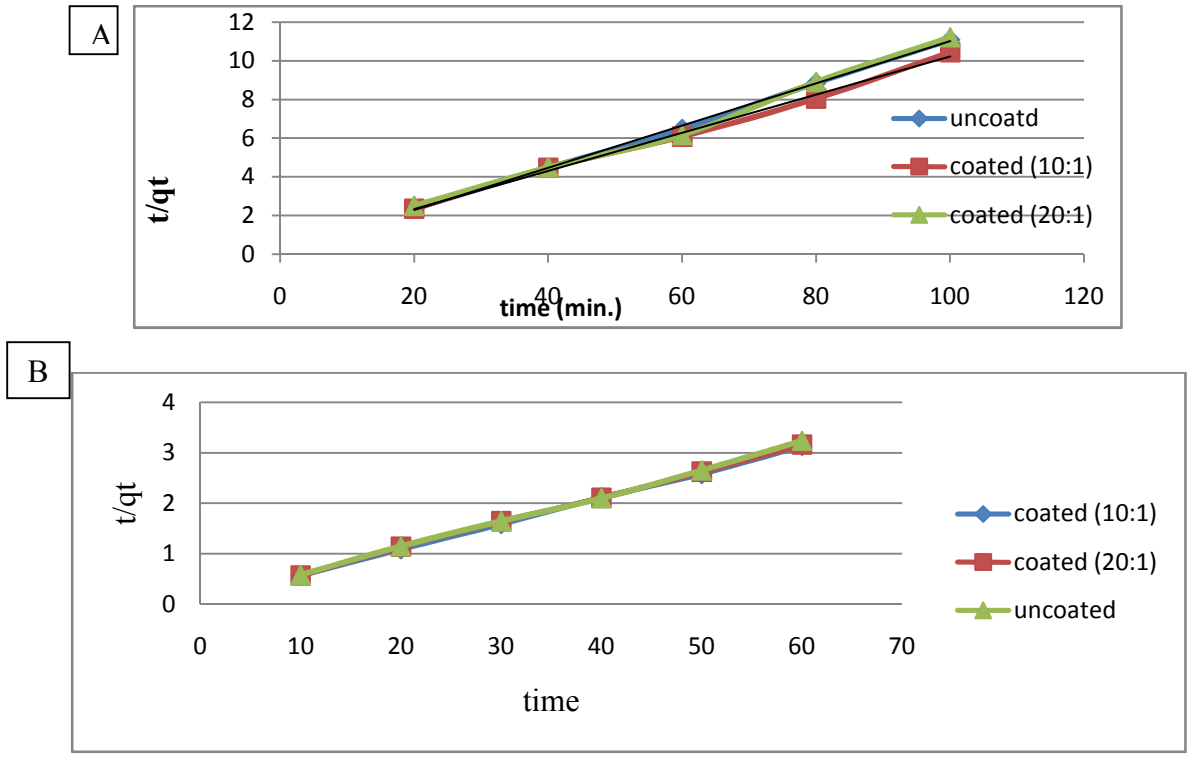

Figure 19. Peseudo 2nd order kinetics at (A). 25 ml of10 mg/l ,(B). 25 ml of 20 mg/l at fixed (dosage = 25 mg , room temprature , shaker speed 100 rpm, PH optimum for all adsorbent) and time (10, 20, 30, 40, 50, 60)min.)

The kinetic parameters and the correlation coefficients (R^2) were determined from nonlinear regression. Fig. 17 and 18 represent for pesedo 1st and 2nd order kinetics respectivly and their parametrs were given in Table 4 .The calculated qe values (qe,cal) of pesedo 2nd order model is close to the experimental ones (qe,exp) as compared to pesedo 1st order kinetics model. The R^2 values also for the pseudo-second-order kinetic model close to 1 which indicates that expermental data were in good greement with pesedo second kinetics order model.

Table 4 Kinetic parameters for the adsorption of MB onto Fe_3O_4 and HA/Fe_3O_4.

Adsorbent type	Concentration(mg/l)	Qe exp.(mg/g)	Pseudo 1st order			Pseudo 2nd order		
			K_1 (min^{-1})	Qe cal.(mg/g)	R^2	K_2 (gmg^1min^{-1})	Qe cal.(mg/g)	R^2
Fe_3O_4	10 mg/l	9.273	-0.013	2.469	0.762	0.0686	9.345	0.998
	20 mg/l	19.02	-0.041	3.07	0.856	0.03864	19.231	0.998
HAC-1	10 mg/l	9.94	-0.079	10.67	0.835	0.027	10.2	0.996
	20 mg/l	19.356	-0.052	2.97	0.944	0.052	19.607	0.999
HAC-2	10 mg/l	9.73	-0.008	1.564	0.562	0.118	9.17	0.993
	20 mg/l	19.04	-0.097	7.2	0.786	0.0283	19.608	0.999

4.2.3. Adsorption isotherms

In order to study how the molecules of MB interact with the adsorbent surface the adsorption isotherms were used to analyze the experimental data. Isotherms study can describe how an adsorbate interacts with adsorbent. The isotherm provides a relationship between the concentration of dye in solution and the amount of dye adsorbed on the solid phase when both phases are in equilibrium. The most widely used isotherm equations are Langmuir and Freundlich equations.

Figure 19 and 20 shows the equilibrium isotherms for the adsorption of MB onto humic acid coated magnetite NPs and uncoated magnetite NPs and the equilibrium adsorption data were analyzed by using the Langmuir and Freundlich isotherm models. The Langmuir model is used to describe the formation of monolayer adsorbate on the outer surface of the adsorbent. The Langmuir isotherm is often applicable to a homogeneous adsorption surface with all the adsorption sites having equal adsorbate affinity, while the Freundlich isotherm described that during the adsorption process different sites of the adsorbent are involved with several adsorption energy is an empirical relation for adsorption over heterogeneous

surfaces. The isotherms based on the experimental data and the parameters obtained from nonlinear regression by both models are shown in Fig. 19 and 20 for Langmuir and Freundlich model respectively.

A)

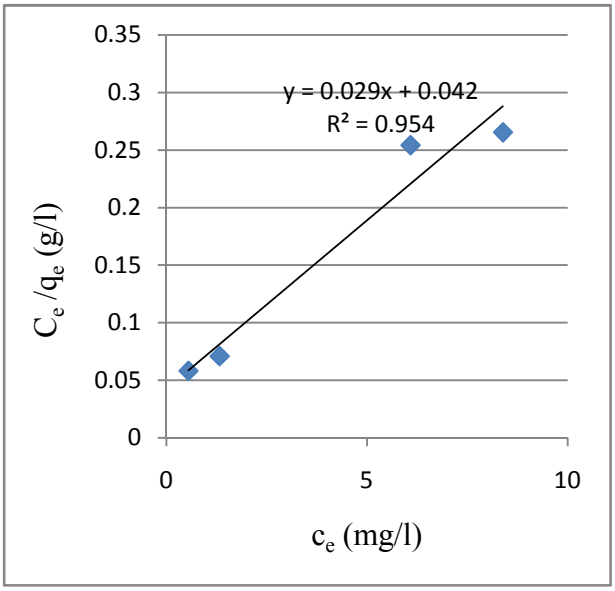

B)

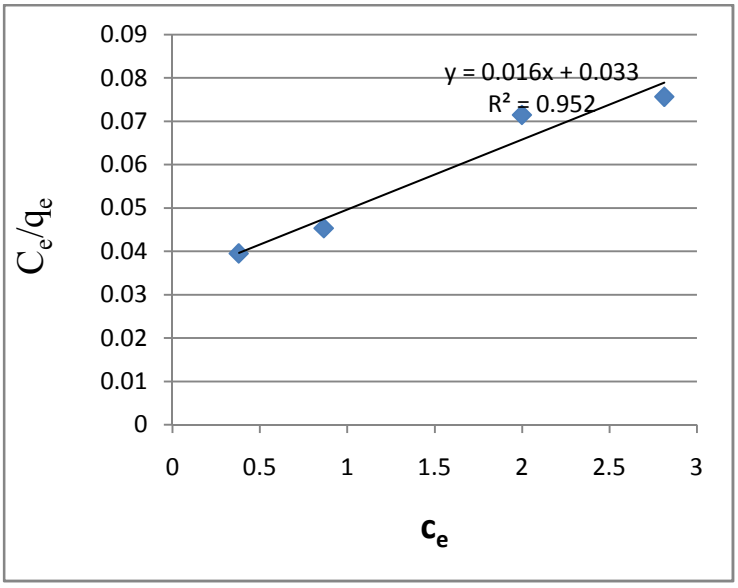

C)

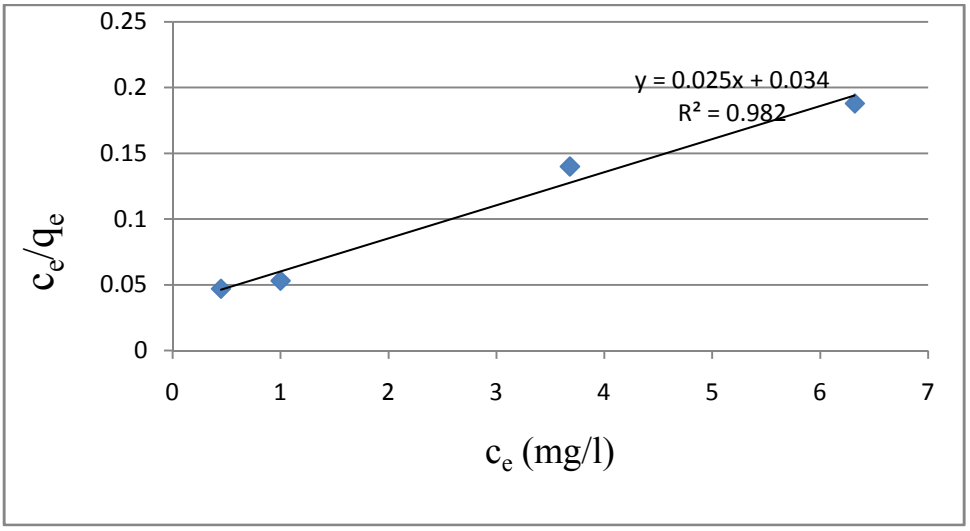

Figure 20.Langmuir isotherm model for different adsorbents (A).Fe_3O_4 ,(B). HAC-1 and (C). HAC-2 at constant dosage (25 mg/l), pH optimum (9 for Fe_3O_4 and HAC-2 , 7 for HAC-1),contact time 60 min, shaker speed 100rpm, room temperature and concentration (10-40 mg/l with in 10mg/l intervals)

The essential characteristics of the Langmuir isotherm can be expressed in terms of a dimensionless constant separation factor R_L given by following relation that can be used to determine the feasibility of adsorption in a given concentration range over adsorbent (Wang Y., et al, 2009).

$$R_L = \frac{1}{1 + bC0} \quad \text{..... (10)}$$

Where b is Langmuir constant related to the energy of adsorption (L mg−1) and C_0 is initial concentration (mg/l) .The calculated RL values at different initial dye concentration were written in the **table 5** below**.** RL value indicates the adsorption nature to be either unfavorable if RL>1), linear if RL =1, favorable if 0< RL<1 and irreversible if RL=0 (McKay G., 1982). For this study all the valves were lies between 0 and 1 which confirming that the adsorption of dye over the adsorbent was favorable.

Table 5 Dimensionless constant separation factor R_L value for different adsorbent at different initial concentration

Adsorbent type	Concentration(mg/l)			
	10 mg/l	20 mg/l	30mg/l	40mg/l
Fe_3O_4 R_L-value	0.1266	0.06757	0.0461	0.03497
HAC-2 R_L-value	0.171	0.0935	0.0643	0.049
HAC-1 R_L-value	0.11976	0.0637	0.0434	0.0329

Freundlich isotherm graphs

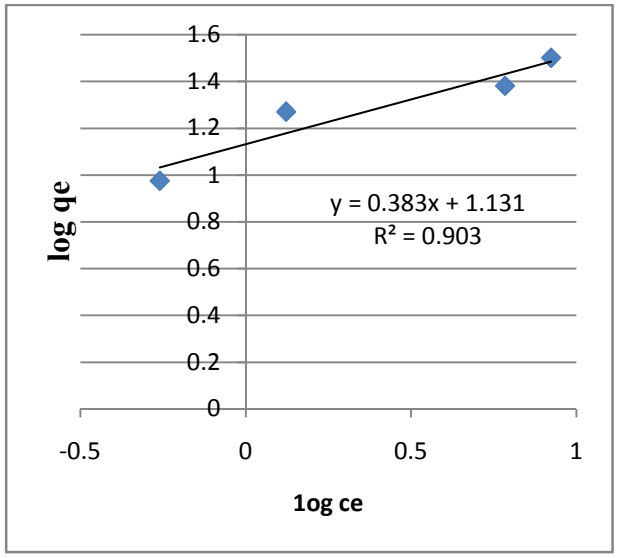

A).

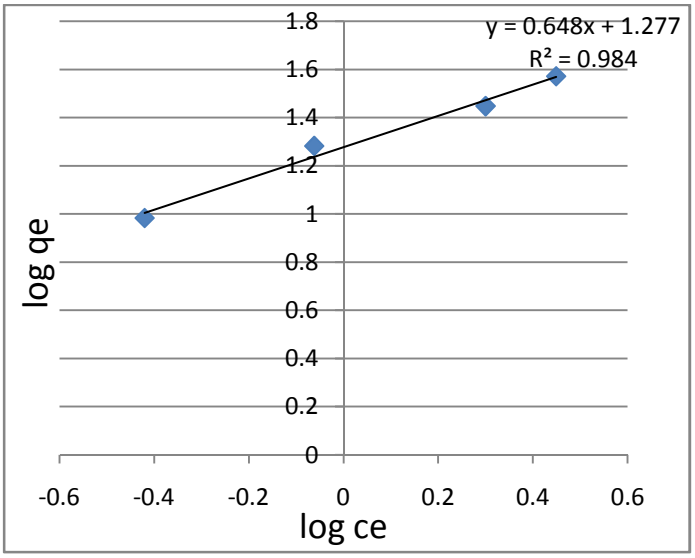

B).

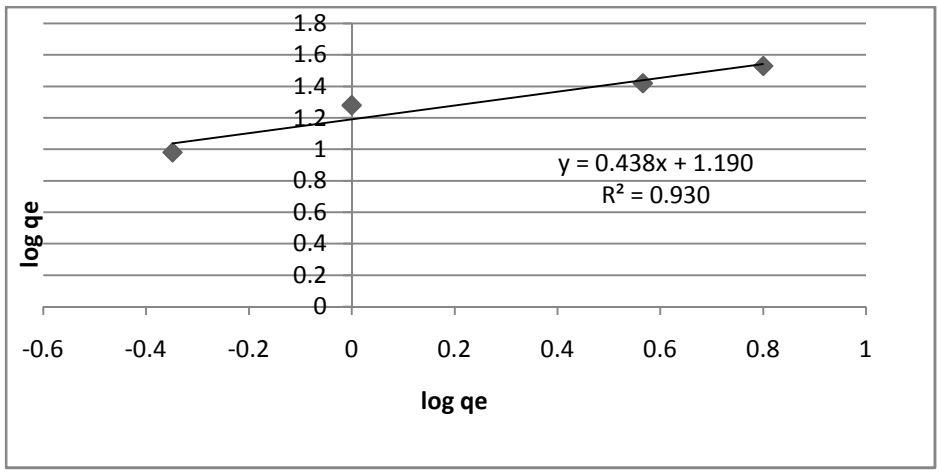

Figure 21. Freundlich isotherm model for different adsorbents (A). Fe_3O_4 , (B). HAC-1and (C). HAC-2 experimental condition similar to Langmuir model.

For the Freundlich isotherm if n = 1 then the partition between the two phases are independent of the concentration. If value of 1/n is below one it indicates a normal adsorption. On the other hand, 1/n being above one indicates cooperative adsorption. For this study as shown in the table 6 the value of 1/n was below 1 for all adsorbents which indicates the normal adsorption. Kf and n are parameters characteristic of the sorbent sorbate system, which must be determined by data fitting and whereas linear regression is generally used to determine the parameters of kinetic and isotherm models.

Based on the above experimental graph the R^2 values of Langmuir model is greater than Freundlich models for Fe_3O_4 and HAC-2 this indicating that the Langmuir model is suitable for describing the adsorption equilibrium of MB onto these adsorbents but for HAC-1 both Freundlich isotherm and Langmuir model can express the adsorbent behavior but When we see mono layer capacity of adsorbent is greater for Langmuir model and the R^2 value had no significant difference. This indicating that the Langmuir model is suitable for describing the adsorption equilibrium of MB onto this adsorbent.

Table 6 Langmuir and Freundlich isotherm model constants and correlation coefficients for adsorption of methylene blue

Adsorbent type	Isotherm	Regression (R^2)	Estimated isotherm parameters
Fe_3O_4	Langmuir	0.954	b = 0.69 L/mg q_m = 34.48 mg/g
	Fredrich	0.903	1/n =0.383 , n = 2.61 K_f = 13.52 mg/g
HAC-1	Langmuir	0.952	b = 0.485 l/mg q_m = 62.5 mg/g
	Freundlich	0.984	1/n = 0.648, n = 1.543 Kf = 18.92 mg/g
HAC-2	Langmuir	0.982	b = 0.735 l/mg q_m = 40 mg/g
	Freundlich	0.930	1/n = = 0.438 , n = 2.283 Kf =15.488

Table 7 Comparison of the adsorption capacity of HA/Fe_3O_4 and Fe_3O_4 obtained in this study with different adsorbents previously used for removal of MB from aqueous solutions.

Type of adsorbent	Adsorbent capacity (mg/g)	References
Fe_3O_4	34.48	The present work
HAC-1	62.5	The present work
HAC-2	40	The presennt work
M-MWCNTs	48.06	Lunhong Ai., et al, 2011
Rice husk	40.59	Vadivelan V., Kumar K., 2005)
Fe(III)/Cr(III) hydroxide	22.8	Namasivayam C., SumithraS., 2005).
Carbonized citrus fruit peel	25.51	Dutta S., et al, 2011
Silkworm exuviae	25.53	Chen H., Zhao J., Dai G.L., 2011).

The adsorption capacity of MB onto humic acid coated magnetite nano particles have higher adsorptive capacity than that of many other previously reported adsorbents, suggesting that the as prepared HA/Fe_3O_4 have great potential application in dye removal from aqueous solution. This is due to high aromatic nature and multi functionality of coating material which helps to remove dyes through $\boldsymbol{\pi\, to \pi}$ interaction with the MB dye molecule and elecrostatically through the interaction between negative charge of adsorbent and positive charge of MB.

Table 8.Comparetion of the adsorption capacity of HA/Fe_3O_4 and Fe_3O_4 obtained in this study with different adsorbents previously used for removal of MB from aqueous solutions at 30mg/l

Adsorbent type	Adsorbent capacity (mg/g)	References
	30 mg/l	
Fe_3O_4	23.92	The present work
HAC-1	28	The present work
HAC-2	26.32	The present work
Chitosan–clay composite	20	Auta, M. & Hameed, B. H., 2014).
Acid modified local clay beads	15	Auta, M. & Hameed, B. H., 2013).
Carbon nanotubes	24	Yao, Y., et al, 2010
Coir pith carbon	6	Kavitha, D., & Namasivayam, C., 2007)
Graphene oxide	31	Liu, T. et al, 2012).

As shown in the above table the removal efficiency of this research work was better than that of the previous work. This was due to small surface area to volume ratio of the synthesized NPs and the multi functional and highly aromatic nature of coating material humic acid.

5. Conclusions and Recommendations

5.1. Conclusions

This study investigated on the synthesis and characterization of humic acid coated magnetite NPs by cooprcipitation method for removal of methylene blue from aqueous solution. HA/Fe_3O_4NPs were successfully synthesized and Humic acids were strongly prevented the aggregation and oxidation of magnetite NPs by electrostatic ally and steric effect respectively. The method used to prepare the HA-Fe_3O_4 NPs was efficient, as shown by the several characterization analyses. The FT-IR spectra and EDX spectra reveal that HA has been successfully coated onto surface of Fe_3O_4 by chemical bond. The result also showed that increasing humic acid controls size, prevent oxidation and increase its capacity removing MB.

For adsorption of MB by nano adsorbents several factors such as MB dye concentration, pH solution; adsorbent dosage and contact time were investigated. The optimum parameter were obtained pH 9 (Fe_3O_4, HAC-2) and 7 for (HAC-1) , initial concentration (10 mg/l) for all, contact time 60 minute for (Fe_3O_4, HAC-2) and 80 minute (HAC-1) and adsorbent dosage 25 mg for all. Based on the removal rate of MB, Fe_3O_4, HAC-2 and HAC-1 shows good adsorbent characteristics for cationic MB dye, with removal efficiency up to 95.9, 97.6 and 99.4 % respectively.

The adsorption isotherms and kinetics were investigated in detail at optimum PH. Langmuir and Freundlich isotherm models were employed to discuss the adsorption behavior. The equilibrium data were better described by Langmuir isotherm model with maximum monolayer adsorption capacity of 34.48 mg g^{-}1,40 mg g−1 and 62.5mg g−1 for Fe_3O_4 , HAC-2 and HAC-1 respectivly. The kinetic study revealed that adsorption process was well fitted the pseudo second order kinetic model. The electrostatic attraction and $\pi - \pi$stacking interactions between Fe_3O_4/HA and MB account for the high adsorptive performance of the Fe_3O_4/HA NPs. The coating material has multifunctional group and highly aromatic nature which leads to increase removal rate of MB. In general this finding demonstrates that Fe_3O_4/HA had higher potential of effective removal of MB dye from aqueous solution.

5.2. Recommendations

Humic acid coated magnetite NPs can also be used as a possible alternative for the removal of other cationic dyes and degradation and adsorption of heavy metal due to its multi functionality of coating material humic acid and the amphoteric nature of magnetite NPs.

Further studies should be carried out by extracting humic acid from the natural source which soil and used as coating material for the nano adsorbent. It is also possible to study the thermodynamics of the system as well as desorption to get a fuller picture of the removal capacity of the Fe_3O_4 /HA for cationic organic dyes and heavy metal removal from different types of wastewater. Other studies should be conducted using this adsorbent like biological activities (antibacterial activities) because both humic acid and magnetite NPs have medicinal applications each individual.

6. References

Adegboyega N.F, Sharma V.K., Siskova K.M.,Vecerova R, Kolar M., R. Zboril R. and Gardea-Torresdey J.L, (2014).Environ. Sci.Technol. 48: PP. 3228–3235.

Ahmed, F., K.Shalendr, A.Nishat, M.S. Anwar, S.Y. Lee, K. Gyung-Suk, P. Dae-Won, H.K. Bon, G.L.Chan., (2011). Preparation and characterizations of polyaniline (PANI)/ZnO nanocomposites film using solution casting method. Thin Solid Films.519: pp. 8375–8378.

Ai L.H., Zhou Y., Jiang J., (2011).Removal of methylene blue from aqueous solution by montmorillonite/CoFe2O4composite with magnetic separation performance, Desalination 266: pp. 72–77.

Ainsworth, C. C., and M. E. Sumner., (1985). Effect of aluminum substitution in goethite on phosphorus adsorption: IL Rate of adsorption. Soil Sci. Soc. Am. J.; 49: pp. 1 149- 1153.

Ainsworth, C. C., J. L. Pilon, P. L. Gassman, and W. G. Van der Sluys., (1994). Cobalt, cadmium, and lead sorption to hydrous iron oxide: Residence time effect. Soi1 Sci. Soc. Am, J.; 58: pp. 1615-1623.

Aitkin R.J, Creely K.S, .Tran C.L, (2004). Nanoparticles: An Occupational Hygiene Review. Research Report 274. Prepared by the Institute of Occupational Medicine for the Health and Safety Executive, *North Riccarton, Edinburgh, England;* 19: pp.113.

Aly, Osman M and Faust, Samuel D., (1987). Adsorption processes for water treatment. *Butterworth Publisher (Boston)* ; pp. 509

Ambashta R.D., Sillanpaa M., (2010). Water purification using magnetic assistance: are views*, J. Hazard. Mater;* 180 (1–3): pp. 38–49.

Anbalagan Krishnasamy, Mohanraj Sundaresan and Pugalenthi Velan, (2015). Rapid phytosynthesis of nano-sized titanium using leaf extract of Azadirachta indica; International Journal of Chem. Tech Research CODEN (USA):,8, No.4: pp. 2047-2052.

Anjaneyulu, Y.; Sreedhara Chary, N. & Suman Raj, D.S., (2005). Decolourization of industrial effluents – available methods and emerging technologies a review. Reviews in Environmental Science and Bio/Technology, Vol.4, pp. 245-273, DOI 10.1007/s11157-005-1246.

Ardejani F. Doulati, Kh. Badii, N. Yousefi Limaee, N.M. Mahmoodi, M. Arami, S.Z. Shafaei, A.R. Mirhabibi., (2007). Numerical modeling and laboratory studies on the removal Adsorption Technique for the Removal of Organic Pollutants from Water and Wastewater of dyes from textile effluents use orange peel, a low-cost adsorbent. *Dyes and Pigments*; 73:pp. 178-185.

Auta, M. & Hameed, B. H., (2013). Acid modified local clay beads as effective low-cost adsorbent for dynamic adsorption of methylene blue. J. Ind. Eng. Chem. 19: pp. 1153–1161.

Auta, M. & Hameed, B. H., (2014). Chitosan clay composite as highly effective and low-cost adsorbent for batch and fixed-bed adsorption of methylene blue. Chem. Eng. J. 237: pp. 352–361.

B. J. Hwang, R. Santhanam, D. G. Liu, J., (2001). Structure stabilization of LiMn2O4 cathode material by bimetal dopants Power Sources, 97-98: pp. 443-446.

Baban, A.; Yediler, A. & Ciliz, N.K., (2010). Integrated water management and CP implementation for wool and textile blend processes. Clean, Vol.38, No.1, and pp. 84-90.

Barr T.L., Modern ESCA.,(2008).The Principles and Practice of X-Ray Photoelectron Spectroscopy, Boca Raton, FL: CRC Press. ; pp. 376.

Beveridge, J.S. et al., (2011). Purification and Magnetic Interrogation of Hybrid Au-Fe(3)O(4) and Fe Pt-Fe(3)O(4) Nanoparticles. Angew Chem. Int Edit 50: pp. 9875-9879.

Birch, R.R.; Biver, C. Campagna, R.; Gledhill, W.E.; Pagga, U.; Steber, J.; Reust, H. & Bontinck, W.J. (1989). Screening of chemicals for anaerobic biodegradability. Chemosphere, 19(11): pp. 1527-1550.

Borggaard, O. K., (1983b). Effect of surface area and mineralogy of iron oxides on their surface charge and anion-adsorption properties. Clays Clay Miner. 3 1: pp. 230-232.

Börnick, H. & Schmidt, T.C., (2006). Amines, In: Organic pollutants in the water cycle. Properties, occurrence, analysis and environmental relevance of polar compounds, T. Reemtsma & M. Jekel, (Eds.), pp. 181-208.

Boutonnet, M., Logdberg, S. & Svensson, E.E., (2008). Recent developments in the application of nanoparticles prepared from w/o micro emulsions in heterogeneous catalysis. Curr Opin Colloid; 13: pp. 270-286.

Brydson R, Brown A., (2008). An investigation of the surface structure of nanoparticulate systems using analytical electron microscopes corrected for spherical aberration. In: Turning Points in Solid-State, Material and Surface Science. London: RSC Publishing, pp. 778– 791.

C. J. Brinker, G. W. Scherer., (1990). Sol - gel science:The Physics and the chemistry of sol gel processing', Academic Press, Inc. London.

Cameron FK. (1915). Soil colloids and the soil solution. *J. Phys Chem*.; 19:pp.1–13.

Cao, S.-W., Zhu, Y.-J., Zeng, Y.-P., (2009). Formation of c-Fe_2O_3hierarchical nanostructures at 500 0 C in a high magnetic field.J. Magn. Magn. Mater. 321: pp. 3057–3060.

Carlos, L., Cipollone, M., Soria, D.B., Moreno, M.S., Ogilby, P.R., Einschlag, F.S.G., Martire, D.O., (2012).The Effect of Humic Acids Binding to Magnetite Nanoparticles on The Photo degradations of Reactive Oxygen Species, Separation and Purification Technology; 91: pp. 23-29.

Carmona A.J., , Carmona M.A., Palomino-Ovandoa Orlando Hernánde Cristobal ,Sánchez-Morac E., Toledo-Solano M., (2017)., Synthesis and characterization of magnetic opal/Fe3O4 colloidal crystal; Journal of Crystal Growth ; 462: PP. 6-11

Chakrabarti, S., Ganguli, D., Chaudhuri, S., (2004). Optical properties ofc-Fe2O3 nanoparticles dispersed on sol-gol silica spheres. J. Physica. E24, pp. 333.

Chen H., Zhao J., Dai G.L., (2011).Silkworm exuviae a new non-conventional and low-cost adsorbent for removal of methylene blue from aqueous solutions, J. Hazard.Mater. 186: pp. 1320–1327

Chen Y., and Aviad T., (1990). Effects of humic substances on plant growth; In: P. McCarthy etal. (Eds.). Humic substances in soil and crop sciences: selected readings. *Amer. Soc. Agronomy, Madison, WI*: pp. 161-186.

Cundy A.B., Hopkinson L, Whit R.L.D., (2008). Use of iron-based technologies in contaminated land and groundwater remediation, A review, *Science of the total Environment*; 400(1–3) : pp 42–51.

Dutta S., Bhattacharyya A., Ganguly A., Gupta S., S. Basu, (2011).Application of response surface methodology for preparation of low-cost adsorbent from citrus fruit peel and for removal of methylene blue, Desalination 275: PP. 26–36

Englert, B. C., (2007). Nanomaterials and the environment: uses, methods and measurement. *Journal of Environmental Monitoring*; 9: pp. 1154-1161.

Etolka tombacz, (2003). The effect of humic acid adsorption on PH dependent surface charging and aggregation of magnetite nanoparticles, *J.colloid interface sc*.;1: pp. 582.

Etolka tombacz, (2003). The effect of humic acid adsorption on PH dependent surface charging and aggregation of magnetite nanoparticles, *J.colloid interface sc*.; 1: pp. 582.

Faraji, M. Yamini Y., and M. Rezaee M., (2010). Magnetic nanoparticles: synthesis, stabilizations, functionalization, characterization and application, *J. Iran. Chem. Soc*; 7: pp. 1-37.

Faraji, M., Yamani, Y. & Rezaee, M., (2010).Magnetic nanoparticles: Synthesis, stabilization, functionalization, characterization, and applications. J Iran Chem. Soc 7: pp. 1-37.

Farmer V. C. Phil. Trans. R. Soc. Lond. A., (1982). Synthesis and characterization of magnetite nanoparticles for the removal of heavy metal from aqueous solutions, 305: pp. 609-619.

Frimmel F.H and Christman R.F, (1988). Humic substances and their role in the environment, 1st ed., *Wiley-Inter-science Publication; New York*; Vol. **1** : pp. 59-74.

Fu L.J. Liu H., Li C.,Wu Y.P.: E. Rahm, R. Holze. H. Q. Wu, (2005). Preparation and characteristic of carbon-coated Li4Ti5O12 anode material Progress in Materials Science 50: pp. 881-928.

Garg V.K, Kumar R, Gupta R., (2004).Removal of malachite green dye from aqueous solution by adsorption using agro-industry waste: a case study of Prosopis cineraria, *Dyes and Pigments* ; 62: pp.1-12.

Griffith J.R., (1981). The Chemisty of Coatings, *Journal of Chemical Education*, 58: pp .956-958

Guo L, Santschi PH. (2006). Ultra filtration and its applications to sampling and characterization of aquatic colloids. In Wilkinson K, Lead J, eds, Environmental Colloids and Particles. John Wiley, Hoboken, NJ, USA; pp. 159–221.

Hanada N., Hirotoshi E., Chikawa T., Akiba E. and Fujii H.,(2008). SEM and TEM characterization of magnesium hydride catalyzed with Ni nano-particle or Nb2O5; J. Alloy Compd.; 450: 395-399.

Heidarizad M., Şengör S.S., (2016). Synthesis of graphene oxide/magnesium oxide nano composites with high-rate adsorption of methylene blue, Journal of Molecular Liquids; 224 pp. 607-617

Howe JM, Mori H, Wang ZL., (2008). In situ high-resolution transmission electron microscopy in the study of nanomaterials and properties. MRS Bull; 33(2): pp.115–121.

Hu C.H, Li J.L, Zhou Y., Li M., Xue F., Li H.M., (2009). Enhanced removal of Methylene Blue from aqueous solution by Pummelo peel pretreated with Sodium Hydroxide, *J. Health Sci*.55(4): pp.619-624.

Huang, S., Chen G., Kong J., (2008). Magnetic removal of dyes from aqueous solution using multi-walled carbon nanotubes filled with Fe2O3 particles, *J.Hazard. Mater*; 160 (2–3): pp. 643–647.

Hui C, Shen C, Tian J, et al., (2011) Core-shell Fe 3 O 4@ SiO 2 nanoparticles synthesized with well-dispersed hydrophilic Fe_3O_4 seeds. Nanoscale. 3(2): PP. 701–705.

Hutten, A.; Sudfeld, D., Ennen, I.; Reiss, G.; Hachmann, W.;Heinemann, U.;Wojczykowski, K.; Jutzi, P.; Saikaly, W.;Thomas, G.,(2004). New magnetic nanoparticles for biotechnology. J. Biotechnology.;112: pp. 47–63.

Hyeon, T., Lee, S.S., Park, J., Chung, Y. & Na, H.B., (2001). Synthesis of highly crystalline and monodisperse Maghemite nanocrystalline without a size-selection process. J Am Chem Soc 123: pp. 12798-12801.

Illes E., and Tombacz E., (2005). The role of variable surface charge and surface complexation in the adsorption of humic acid on magnetite, *J. Colloid Surf, A*; 203: pp. 99-109.

Illes E., and Tombacz E., (2006). The effect of humic acids adsorption on pH-dependent surfece charging aggregation of magnetic nanoparticles, J. *Colloid Surf, A;* 295: pp.115-123.

Indira T.K, Lakshmi P.K., (2010). Magnetic Nanoparticles: A review. Int. J. Pharm. *Sci. & Nanotechnology*; 3(3): pp.1035-1042.

Jain T.K, Morales M. a, Sahoo S.K, D. L. Leslie-Pelecky and V. Labhasetwar, (2005). Magnetic Nanoparticles for Power Absorption: optimizing size, shape and magnetic Properties, Molecular *Pharmaceutics*; 2: pp.194.

Jain TK, Reddy MK, Morales MA, Leslie Pelecky DL, Labhasetwar V., (2008). Biodistribution, clearance, and biocompatibility of iron oxide magnetic nanoparticles in rats. Mol Pharm.; 5(2):pp.316–327.

Jolivet J. P, Chanéac C. and Tronc E., (2004). Iron oxide chemistry. From molecular clusters to extended solid networks, *Chemical Communications*; 10: PP. 481-487.

Kavitha, D., & Namasivayam, C., (2007), Experimental and kinetic studies on methylene blue adsorption by coir pith carbon. Bioresour. Technol. 98: pp.14–21.

Kim, D.K., Zhang, Y., Voit, W., Rao, K.V., & Muhammed, M., (2001 Synthesis and characterization of surfactant-coated superparamagnetic monodispersed iron oxide nanoparticles. J Magn Magn Mater; 225: pp. 30-36.

Kurniawan, T. A. and Lo, W.H., (2009). Removal of refractory compounds from stabilized landfill leachate using an integrated H_2O_2 oxidation and granular activated carbon (GAC) adsorption treatment. *Water Research*; 43: PP. 4079-4091.

Laurent S, Forge D., Port M., Roch A, Robin C., Vander L.Elst. And Muller R.N., (2008). , Magnetic iron oxide nanoparticles: Synthesis, stabilization, vectorization, physic chemical characterizations and biological applications, *Chemical Reviews*; 108: pp. 2064-2110.

Lead JR, Davison W, Hamilton-Taylor J, Buffle J. 1997. Characterizing colloidal material in natural waters. Aquatic Geochemistry3:213–232.

Lead JR, Wilkinson KJ.,(2006). Environmental colloids: Current knowledge and future developments. In Wilkinson KL, Lead JR, eds, Environmental Colloids: Behavior, Structure and Characterization. *John Wiley, Chichester, UK*, pp. 1–15.

Li, Y., Afzaal, M. & O'Brien, P., (2006). The synthesis of amine-capped magnetic (Fe, Mn, Co, Ni) oxide nanocrystals and their surface modification for aqueous dispersibility. J Mater Chem 16: pp. 2175-2180.

Lian, S.Y. et al. (2004). Synthesis of magnetite nanorods and porous hematite nanrods. Solid

Liu Y, Guo S., Zhang Z., Huang W, D. Baigl, M. Xie, Y. Chen, D. Pang, (2007). A micro pillar integrated smart micro fluidic device for specific capture and sorting of cells Electrophoresis; 28(24): pp. 4713-4722.

Liu Z.L., Deng J.C., Deng J.J. and LiF.F., (2008).Materials Science and Engineering B-Advanced Functional Solid-State Materials; Fabrication and photo catalysis of CuO/ZnO nano-composites via a new method; 150: pp. 99-104.

Liu, T. et al, (2012). Adsorption of methylene blue from aqueous solution by grapheme. Colloid. Surface. B. 90: pp. 197–203.

LopezPerez, J.A., LopezQuintela, M.A., Mira, J. & Rivas, J., (1997). Preparation of magnetic fluids with particles obtained in micro emulsions. Ieee T Magn 33: pp. 4359-4362.

Lu, A.H. et al., (2004).Nano engineering of a magnetically separable hydrogenation catalyst. Angew Chem Int Edit 43: pp. 4303-4306.

Lu, A.H., Salabas,E.L.& Schuth, F., (2007). Magnetic nanoparticles: Synthesis, protection, functionalization, and application. Angew Chem. Int Edit 46: pp.1222-1244.

Lunhong Ai, Chunying Zhang, Fang Liao, Yao Wang Ming Li Lanying Meng ,Jing Jiang , (2011). Removal of methylene blue from aqueous solution with magnetite loaded multi-wall carbon nanotube: Kinetic, isotherm and mechanism analysis, Journal of Hazardous Materials; 198:pp. 182 -190.

M R Joya1, J Bar´on-Jaimez and J Barba-Ortega,(2013). Preparation and characterization of F e_2O_3Nanoparticles, Journal of Physics: Conference Series pp. 466

Maeda M. Kuroda C.S., Shimura T., Tada M., and Abe M. Yamamuro S. and Sumiyama K. H. Handa J., (2006). Probing magnetic interactions in columnar phases of a paramagnetic gold dithiolene complex .Appl. Phys. 99: 08H103.

Maity D. and Agrawal C., (2007). Synthesis of iron oxide nanoparticles under oxidizing environment and their stabilization in aqueous and non-aqueous media*, J. Mag.Magn. Mater*; 308: pp. 46-55.

Maity D., and Agrawal C., (2007). Synthesis of iron oxide nanoparticles under oxidizing environment and their stabilization in aqueous and nonaquoeous media, *J. Mag.Magn.Mater*., 308: pp. 46-55.

Maity, D.;Agrawal, D. C., (2007). Synthesis of iron oxide nanoparticles under oxidizing environment and their stabilization in aqueous and non-aqueous media's. *Magn. Magn. Mater*; 308: pp. 46–55

Mauter, M. S.; Elimelech, M., (2008). Environmental applications of carbon-based nanomaterials. *Environmental Science & Technology*; 42, (16): pp. 5843-5859.

McKay G., (1982). Adsorption of dye stuffs from aqueous solution with activated carbon. I. Equilibrium and batch contact time studies, J. Chem. Technol. Biotechnol. 32: PP. 759–772.

Murray C.B., Kagan C.R. and Bawendi M.G., (1995). Self-Organization of CdSe Nanocrystalline into Three-Dimensional Quantum Dot Super lattices; Science; ; 270: 1335-1338.

Namasivayam C., Sumithra S., (2005). Removal of direct red 12B and methylene blue from water by adsorption onto Fe (III)/Cr (III) hydroxide, an industrial solid waste, J. Environ. Manage. 74: PP .207–215.

Namasivayam C., Sumithra S., (2005). Removal of direct red 12B and methylene blue from water by adsorption onto Fe (III)/Cr (III) hydroxide, an industrial solid waste, J. Environ. Manage. 74: PP .207–215.

National Nanotechnology Initiative. (2009). What Is Nanotechnology? (http://www.nano.gov/html/facts/whatIsNano.html).

Ogner G., and Schnitzler M., (1970). Humic substances: Fulvic acid-dialkyl phthalate complexes and role in pollution, *Journal of Science; vol*. **170**, no. 3955:pp 317-318.

Park, J. et al. (2004). Ultra-large-scale syntheses of monodisperse nanocrystals. Nat Mater 3 : pp. 891-895.

Perez, S.; Farre, M.; Barceló, D., (2009). Analysis, behavior and ecotoxicity of carbon-based nanomaterials in the aquatic environment. *TracTrends Anal. Chem*.; 28, (6): pp. 820-832.

Perkampus H.H.,, V-VIS spectroscopy and its applications. Springer-Verlag: Berlin ; (1994).New York, pp. 244.

Petcharoen K, Sirivat A., (2012). Synthesis and characterization of magnetite nanoparticles via the chemical co-precipitation method. *Mater Sci Eng B*.; 177(5): pp.421–427.

Petcharoen, K., and Sirivat, A., (2012). Synthesis and characterization of magnetite nanoparticles via the chemical co-precipitation method, Mater.Sci. Eng., B, 177 (5): pp. 421–427.

Pokroy B., Kang S.H.,, Mahadevan L., and Aizenberg, J. (2009). Self-Organization of a Mesoscale Bristle into Ordered, Hierarchical Helical Assemblies," Science, 323: pp. 237-240.

Qadri S., Ganoe A., Haik Y., (2009). Removal and recovery of acridine orange from solutions by use of magnetic nanoparticles , J. Hazard. Mater. 169 (1–3): PP. 318–323.

Qadri S., Ganoe A., Haik Y., (2009). Removal and recovery of acridine orange from solutions by use of magnetic nanoparticles , *J. Hazard. Mater*. ;169 (1–3): pp. 318–323.

Rajabia A., Yaminia Y.,*Faraji M., and Nourmohammadian F., (2016). Modified magnetite nanoparticles with cetyltrimethyl ammonium bromide as superior adsorbent for rapid removal of the disperse dyes from wastewater of textile companies, Nano. Chem. Res., 1(1): pp.49-56.

Rehman R., Anwar J. Mahmud M.Salma T.,and Shafique U., (2011). Influence of Operating Conditions on the Removal of Brilliant Vital Red Dye from Aqueous Media by Biosorption using Rice Husk"Journal of Chemical Society of Pakistan, Vol. 33, No. 4 pp. 25-30.

Sajab, M.S. Chia, C.H. Zakaria S., Khiew P.S., (2013) Cationic and anionic modifications of oil palm empty fruit bunch fibers for the removal of dyes from aqueous solutions, Bioresource Technology 128: pp. 571-577.

Salabas Lu, A.H.; E.L.; Schuth, F.,(2007). Magnetic nanoparticles: Synthesis, protection, functionalization, and application. *Angew. Chem. - Int. Edit*.; 46: pp. 1222–1244.

Satoshi H., Nick S. (2013). Microwaves in nanoparticles synthesis: fundamentals and applications, *Wiley-VCH Verlag GmbH, Co. KGaA*; pp. 1-24.

Schwarzer H.C and Peukert W., (2004). Tailoring particle size through nanoparticles precipitation, *Chemical Engineering Communications*; 191:pp.580-606.

Schwarzer H.C and Peukert W., (2004). Tailoring particle size through nanoparticles precipitation, *Chemical Engineering Communications*; 191:pp.580-606.

Schwertmann, U., Gasser U., and Sticher H., (1989). Chromium for iron substitution in synthetic goethites. Geochim. Cosmochim. Acta; 53: pp. 1293- 1297.

Shi JP, Evans DE, Khan AA, Harrison RM. (2001). Sources and concentration of nanoparticles (nm diameter) in the urban atmosphere. *Atmos. Environ.*; 35:1193–1202

Shiva Dehghan Abkenar, (2016). Application of Magnetic-modified Fe_3O_4Nanoparticles for Removal of Crystal Violet from Aqueous Solution: Kinetic, Equilibrium and Thermodynamic Studies, *Journal of Applied Chemical Research*; Iran 10: pp.65-74.

Silverstein RM and Webster FX, Ed.v, (2002). Spectrometric Identification of Organic, Compounds, 6th Edn, Jhon Wiley, and Sons, New York:71-109: p. 72- 126.

Soerja Koesnarpadi, Sri Juari Santosa Dwi Siswanta Bambang Rusdiars, (2017). Synthesis and characterizatation of magnetite nanoparticle coated humic acid (Fe3O4/HA; Procedia Environmental 12 Sciences 30: pp. 103-108.

State Commun 129: pp. 485-490.

Stevenson F.J., (1982). Humus chemistry, Genesis, Composition, Reactions, *John Wiley & Sons, New York*; 18: pp .443.

Sue, K., Kimura, K. & Arai, K.,(2004) Hydrothermal synthesis of ZnO nanocrystals using micro reactor. Mater Lett 58: PP. 3229-3231.

Takafuji, M., Ide, S., Ihara, H. & Xu, Z.H., (2004). Preparation of poly (1-vinylimidazole)-grafted magnetic nanoparticles and their application for removal of metal ions. Chem Mater 16: pp. 1977-1983.

Teja A.S, and Koh P.Y.,(2009). Synthesis, properties, and applications of magnetic iron oxide nanoparticles', Progr. Cryst. Growth Charact. Mater; 55: pp. 22–45.

Teja, A.S. & Koh, P.Y., (2009). Synthesis, properties, and applications of magnetic iron oxide nanoparticles. Prog Cryst Growth Ch 55: pp. 22-45.

Tombacz, E, Horvat, M., and Illes, E., (2006).Magnetite in aqueous medium: coating its surface and surface coated with it, Rom.Rep.Phys. 58: pp.281-286.

Vadivelan V., Kumar K., (2005). Equilibrium, kinetics, mechanism, and process design for the sorption of methylene blue onto rice husk, J. Colloid Interface Sci. 286: pp. 90–100.

Vidal-Vidal, J., Rivas, J. & Lopez-Quintela, M.A.,(2006) Synthesis of monodisperse Maghemite nanoparticles by the microemulsion method. Colloid Surface A 288: pp. 44-51.

Wang H, Zhou A, Peng F, Yu H, Yang J., (2007). Mechanism study on adsorption of acidified multi-walled carbon nanotubes to Pb (II). J. *Colloid Interface Sci.*; 316: pp.277–283.

Wang Y., He X., Wang K., Zhang X., Tan W.,) 2009). Barbated Skullcup herb extract-mediated biosynthesis of gold nanoparticles and its primary application in electrochemistry.J. Colloid Interface Sci., 2009, 73:pp. 75–79.

Wang, M.D., D.Y. Zhu, Y. Liu, L. Zhang, C.X. Zheng, Z.H. He, D.H. Chen and L.S. Wen, (2008).Determination of thickness and optical constants of ZnO thin films prepared by filtered cathode vacuum arc deposition. chinese physics letters,25(2): pp. 743-746

Weber T.W., R.K., (1974). Chakravorti R.K., Pore and solid diffusion models for fixed-bed absorbers, AIChE J. 20:PP. 228–238.

Weber T.W., R.K., (1974). Chakravorti R.K., Pore and solid diffusion models for fixed-bed absorbers, AIChE J. 20: PP. 228–238.

Wei Y. Han B., Hu X., Lin Y., Wang X., Deng X., (2012). Synthesis of Fe_3O_4 nanoparticles and their magnetic properties, *Procedia Eng*.; 27: pp. 632-637.

Xia T, Wang J, Wu C, et al., (2012). Novel complex-cooprcipitation route to form high quality triethanolamine-coated Fe_3O_4 nanocrystals: their high saturation magnetizations and excellent water treatment properties. *CrystEngComm.* ; 14(18):pp.5741–5744.

Y ongchao Li, Z. X., (2013). Stabilization of Fe for Enhanced Transport and Remediation of Hexavalent Chromium in Groundwater. *College of Environmental Science and Engineering, Nankai University*, pp.1-20.

Yao, Y., Xu, F., Chen, M., Xu, Z. & Zhu, Z., (2010). Adsorption behavior of methylene blue on carbon nanotubes. Bioresour. Technol. 101:pp. 3040–3046.

Zhang J.Z., Wang Z.L., Liu J., Chen S. and Liu G.-y., (2003) Self-assembled Nanostructures. Nanoscale Science and Technology, New York: Kluwer Academic/Plenum Publishers.2003; pp. 316.

7. Appendix

7.1. Raw data

Table 9.The result of the effect of pH adsorption for different adsorbent

Type of adsorbent	PH	Absorbance for supernatant (T1)	Absorbance for supernatant (T2)	Average	Ce (mg/l)	Qe (mg/g)	% Removal
Fe_3O_4	3	0.52	0.48	0.5	3.329	11.16	66.7%
	7	0.43	0.42	0.425	2.556	12.49	74.4
	8	0.39	0.37	0.38	2.093	13.17	79.07
	9	0.336	0.305	03205.	1.479	14.2	85.2
	11	0.341	0.337	0.339	1.67	13.88	83.3
HAC-2	3	0.406	0.407	0.4065	2.37	12.762	76.28
	7	0.258	0.256	0.257	0.8247	15.29	91.7
	8	0.262	0.259	0.261	0.866	15.22	91.3
	9	0.23	0.232	0.231	0.556	15.738	94.4
	11	0.584	0.639	0.6115	4.479	9.2	55.2
HAC-1	3	0.291	0.338	0.3145	1.1417	14.3	85.8
	7	0.198	0.224	0.216	0.402	16	96
	8	0.307	0.31	0.29	1.1649	14.73	88.35
	9	0.248	0.246	0.247	0.7216	15.464	92.8
	11	0.491	0.537	0.517	3.505	10.825	64.9

Table 10. Effect of adsorbent dose

Type of adsorbent	Adsorbent Dosage (mg/g)	Absorbance for supernatant (T1)	Absorbance for supernatant (T2)	Average	Ce (mg/l)	Qe (mg/g)	% Removal
Fe_3O_4	10	0.383	0.376	0.3795	2.13	19.675	78.7
	15	0.345	0.352	0.349	1.77	13.7	82.3
	20	0.236	0.24	0.238	0.628	11.715	93.72
	25	0.213	0.22	0.2165	0.407	9.59	95.9
	30	0.235	0.24	0.2375	0.623	7.8	93.7

HAC-2	10	0.273	0.279	0.276	1.02	22.448	89.7
	15	0.269	0.275	0.272	0.9794	15	90.2
	20	0.247	0.196	0.2215	0.45876	11.926	95.4
	25	0.201	0.19	0.2	0.237	9.76	97.6
	30	0.233	0.235	0.234	0.5768	7.844	94.12
HAC-1	10	0.2618	0.258	0.2599	0.854	22.86	91.45
	15	0.248	0.239	0.2435	0.6856	15.524	93.14
	20	0.223	0.218	0.2205	0.448	11.94	95.52
	25	0.2	0.197	0.1985	0.22	9.78	97.8
	30	0.22	0.205	0.2125	0.3659	8.02	96.3

Table 11.Effect of initial concentration

Type of adsorbent	concentration (mg/l)	Absorbance for supernatant (T1)	Absorbance for supernatant (T2)	Average	Ce (mg/l)	Qe (mg/g)	% Removal
Fe_3O_4	5	0.25	0.23	0.24	0.237	4.206	84.12
	10	0.237	0.224	0.2305	0.55	9.45	94.5
	20	0.301	0.31	0.3055	1.324	18.676	93.37
	30	0.783	0.752	0.7675	6.08	23.92	79.7
	40	0.98	1	0.99	8.38144	31.62	79
HAC-2	5	0.22	0.2	0.21	0.34	4.66	93.2
	10	0.223	0.218	0.2205	0.4485	9.55	95.5
	20	0.276	0.272	0.274	1	19	95
	30	0.579	0.489	0.534	3.68	26.32	87.73
	40	0.78	0.8	0.79	6.319	33.68	84.2
HAC-1	5	0.21	0.19	0.2	0.237	4.763	95.25
	10	0.21	0.218	0.214	0.38	9.618	96.18
	20	0.257	0.265	0.261	0.8659	19.13	95.67
	30	0.364	0.382	0.373	2	28	93.3
	40	0.46	0.44	0.45	2.814	37.186	92.9

Table 12. Effect of contact time

Type of adsorbent	Contact time (minute)	Absorbance for supernatant (T1)	Absorbance for supernatant (T2)	Average	Ce (mg/l)	Qe (mg/g)	% Removal
Fe_3O_4	20	0.314	0.332	0.323	1.505	8.494	84.94
	40	0.3	0.26	0.28	1.06	8.938	89.38
	60	0.263	0.232	0.2475	0.7268	9.273	92.73
	80	0.271	0.268	0.2695	0.9536	9.04	90.04
	100	0.274	0.269	0.2715	0.974	9.0	90
HAC-2	20	0.385	0.369	0.377	2	8	80
	40	0.269	0.3	0.2845	1.1	8.9	89
	60	0.198	0.208	0.203	0.268	9.73	97.3
	80	0.285	0.267	0.276	1.02	8.98	89.8
	100	0.293	0.273	0.283	1.09	8.91	89.1
HAC-1	20	0.313	0.333	0.323	1.505	8.494	84.94
	40	0.29	0.27	0.28	1.06	8.938	89.38
	60	0.192	0.189	0.1905	0.139	9.86	98.6
	80	0.181	0.185	0.183	0.06	9.94	99.4
	100	0.217	0.219	0.218	0.42	9.577	95.77

Table 13 .Result of kinetics experiment at concentration of 20 mg/l dosage= 25mg, PH= optimum for both , room temperature and shaker speed 100 rpm.

Type of adsorbent	Contact time (minute)	Ct (mg/l)	Qt (mg/g)	Qe -qt	ln(qe –qt)	t/qt
Fe_3O_4	10	2.814	17.18	1.84	0.6097	0.582
	20	2.608	17.39	1.63	0.489	1.15
	30	1.7835	18.216	0.804	-0.2182	1.647
	40	0.9796	19.02	0	-	2.1
	50	1.1649	18.838	0.182	-1.704	2.654
	60	1.47	18.525	0.495	-0.703	3.2388
HAC-2	10	2.608	17.39	1.65	0.5	0.575
	20	2.485	17.515	1.525	0.422	1.142
	30	1.753	18.247	0.793	-0.232	1.644
	40	1.04	18.96	0.08	-2.5257	2.1097

	50	0.958	19.04	0	-	2.626
	60	1	19	0.04	-3.22	3.158
HAC-1	10	2.495	17.5	1.856	0.62	0.57
	20	1.66	18.34	1.016	0.016	1.091
	30	1.124	18.876	0.48	-0.734	1.59
	40	1.062	18.94	0.416	-0.877	2.112
	50	0.464	19.356	0	-	2.583
	60	0.866	19.03	0.226	-1.487	3.136

Table 14.Result of kinetics experiment at concentration of 10 mg/l dosage= 25mg, PH= optimum for both, room temperature and shaker speed 100 rpm

Type of adsorbent	Contact time (minute)	Ct (mg/l)	Qt (mg/g)	Qe -qt	ln (qe –qt)	t/qt
Fe_3O_4	20	1.505	8.494	0.779	-0.25	2.354
	40	1.06	8.938	0.335	-1.094	4.475
	60	0.7268	9.273	0	-	6.47
	80	0.9536	9.04	0.233	-1.457	8.849
	100	0.974	9	0.247	-1.398	11.08
HAC-2	20	2	8	1.73	0.548	2.5
	40	1.1	8.9	0.83	-0.186	4.494
	60	0.268	9.73	0		6.1665
	80	1.02	8.98	0.75	-0.2876	8.91
	100	1.09	8.91	0.82	0.2	-0.0862
HAC-1	20	1.505	8.495	1.445	0.368	2.354
	40	1.06	8.938	1.002	0.001998	4.475
	60	0.139	9.86	0.06	-2.813	6.085
	80	0.06	9.94	0		8.05
	100	0.42	9.577	0.363	-1.03	10.44

Table 15. Results for isotherm models at different concentrations

Type of adsorbent	Concentration (mg/l)	Ce (mg/l)	Qe (mg/g)	Log Ce	Log qe	Ce/qe
Fe_3O_4	10	0.55	9.45	-0.26	0.975	0.0582
	20	1.324	18.676	0.122	1.27	0.071
	30	6.08	23.92	0.784	1.38	0.254
	40	8.384	31.62	0.923	1.5	0.2652
HAC-2	10	0.4485	9.55	-0.3481	0.98	0.047
	20	1	19	0	1.28	0.053
	30	3.68	26.32	0.566	1.42	0.1398
	40	6.319	33.68	0.8	1.53	0.188
HAC-1	10	0.38	9.618	-0.42	0.983	0.0395
	20	0.866	19.13	-0.062	1.282	0.0453
	30	2	28	0.3	1.4472	0.0714
	40	2.814	37.2	0.449	1.571	0.0756